## SPECIFIC SURFACE OF FIBROUS MATERIALS

and

### PROBLEMS OF EXPLOSIVES PRODUCTION

bу

Ernest James Wiggins, B.Sc.

A thesis submitted to the Faculty of Graduate Studies and Research at McGill University in partial fulfilment of the requirements for the degree of Doctor of Philosophy.

McGill University, April, 1946 Montreal. P.Q.

#### ACKNOWLEDGEMENT

The author wishes to express his sincere appreciation to

Dr. O. Maass

Dr. W. B. Campbell

and

Dr. J. H. Ross

for their constant interest and encouragement and for their valuable suggestions during the supervision of this work.

Acknowledgement is made to the Canadian Pulp and Paper Association and to the National Research Council for the award of scholarships during the course of this work.

The writer also wishes to express his thanks to Dr.

A. P. Stuart for his collaboration on all investigations of the gas permeability method.

# TABLE of CONTENTS

Part Ia Liquid Permeability Measurements	Page
General Outline	. 1
Historical Review and Introduction	5
Experimental Procedure and Results	31
(a) Equipment and General Procedure	. 31
(b) Measurements with Screen-Classified Sand	35
(c) Measurements with Small Glass Rods	41
(d) Measurements with Copper Wire	42
(e) Measurements with Glass Wool	42
(f) Measurements with Corning Fiberglass	44
(g) Measurements with Mixture of Glass Fibers	46
(h) Measurements with Celanese Yarn	47
(i) Discussion of Results	48
(j) Refinements of Technique for Routine Measurement of Liquid Permeability	53
(k) Construction of Nomographs for Liquid Permeability Data	55
Part Ib Gas Permeability Measurements	
Introduction	67
Experimental Procedure and Results	71
(a) Apparatus and General Procedure	71
(b) Calculation of Specific Surface from Gas Permeability Data	74
(c) Measurements with Corning Fiberglass	. 77

# TABLE of CONTENTS (cont)

<b>5</b> 0
<b>3</b> 0
<b>3</b> 4
<b>3</b> 7
93
94
06
06
L1
12
12
L3

Ph.D. Chemistry

#### Ernest James Wiggins

# Specific Surface of Fibrous Materials and

#### Problems of Explosives Production

A derivation of the Kozeny equation relating specific surface and permeability of a bed of unconsolidated particles is given in detail. The equation is applied to liquid permeability measurements with sand, glass rods, copper wire, glass wool, fiberglass and celanese fibers. Close agreement is obtained between the specific surfaces calculated from permeability data and from the geometry of the particles.

Comparisons are made of gas and liquid permeability measurements with fiberglass, wool fibers, acetylene
black and respirator filter pads. Satisfactory correlation is obtained for all materials except acetylene black.
An analysis of the effects of stationary surface layers of
fluid is given to indicate the upper specific surface limit
for the liquid permeability method.

Methods are described for preparation of carbamite from crude ethylaniline and for purification of the product.

#### SUMMARY

A detailed derivation is given for the Kozeny equation, which relates the permeability to fluids and the specific surface of a bed of unconsolidated particles. The equation was first applied to liquid permeability measurements with beds of near-spherical particles to repeat the work of previous investigators. The equation was then applied to liquid permeability measurements with particles departing increasingly from spherical form. Slender glass rods, copper wire, glass wool, Corning fiberglass and celanese fibers were employed for this purpose. Close agreement was obtained in all cases between the specific surfaces calculated from permeability data and from the geometry of the particles. The results of this investigation indicated that the liquid permeability method provided a means of determining the specific surface of materials closely approaching natural fiber dimensions.

An analysis of the effects of stationary surface layers of fluid indicated the existence of an upper limit of usefulness of the liquid permeability method. However, the same analysis indicated that gas permeability measurements could be used for much higher specific surface ranges, as a result of the lesser thickness of the stationary layers. Gas and liquid permeability measurements were made with fiberglass, natural wool, acetylene black and respirator filter

pads. Satisfactory agreement was obtained between the two methods for all materials except acetylene black. Gas permeability measurements with samples of respirator charcoal showed correlation between the calculated specific surface and the effectiveness of the charcoal. The gas permeability method was found to possess manipulative advantages in measurements with fine particles or with fibrous materials.

Investigations were conducted on the preparation of carbamite from crude ethylaniline. The I.C.I. and duPont processes were found to be satisfactory for this purpose. Preliminary stripping of the crude ethylaniline for removal of sulphur compounds was found to simplify the purification of the reaction product.

#### CLAIMS to ORIGINAL RESEARCH

The Kozeny equation has been shown to be applicable to particles approaching natural fibers in dimensions. This equation relates the specific surfaces of beds of unconsolidated particles and their permeabilities to gases or liquids. A comparison has been made of gas and liquid permeability measurements as means of determining specific surfaces. Close agreement has been obtained between the two methods and the true specific surface for materials such as fiberglass.

An analysis of the effects of stationary fluid layers has been made which indicates the existence of an upper limit of usefulness for the liquid permeability method. A similar investigation for the gas permeability method was not completed, since measurements of the surface areas of military materials were undertaken at that time. The permeability method has been shown to be of value in indicating the effectiveness of respirator filter pads and charcoals.

The preparation of carbamite from crude ethylaniline of Canadian manufacture has been investigated.

# PART I

Specific Surface of Fibrous

Materials.

#### PART Ia

#### GENERAL OUTLINE

The problem of determination of the surface area of irregularly shaped particles has been the subject of attention of a great many investigators. This interest may be attributed on the one hand to the many practical applications of such information, and on the other to the elucidation of fundamental principles which has resulted from the varied and ingenious methods devised.

Applications of surface area determinations to industry may be enumerated almost without limit. The completeness and speed of setting of cement is proportional to the specific surface, pulverized fuels are finely ground to provide a large surface for combustion, and the work done in grinding is itself a function of the new surface created. Powders used as fillers in plastics impart strength to the whole mass by virtue of their large specific surfaces.

The surface areas of fibrous materials are of particular interest throughout the asbestos, textile, pulp and paper industries. For example, the variation in the properties of paper sheets formed from pulps which have undergone different beating treatment may well be explained by the resulting change in surface area available for bonding between fibres during sheet formation. Industries engaged

in processing fibrous materials have long recognized the need for more detailed information about the physical characteristics of their products. While a great multiplicity of testing instruments and methods has been devised, it must be admitted that few of these give an approach to the measurement of any specific physical property. Rather, various subjective properties are measured which are related but distantly to the fundamental characteristics and usually unite several of these in involved relationships. Hence the provision of a reliable means for measuring such an important single physical property as specific surface could scarcely fail to be of interest.

As indicated above, a great variety of methods has been devised for the determination of specific surface. The majority, however, suffer from tediousness and limited applicability. Fortunately, a new means of approach has recently been provided which proves to be subject to almost no limitations as to size or shape of particles, and which is simple, speedy and reliable. Briefly, this new method involves the determination of the permeability of a sample of the material to a fluid of known viscosity. The specific surface of the material may then be calculated by the use of an equation first proposed by J. Kozeny (1, 2). The

presence of a range of sizes or a variety of shapes for the constituent particles detracts nothing from the simplicity or accuracy of the method.

The "Kozeny equation", developed on a theoretical basis to relate permeability of sands to their specific surface, was first applied by Carman (3, 4) to the problem of determination of specific surface from permeability data. In the course of his investigations, Carman demonstrated the correctness of Kozeny's relation for a wide variety of particle shapes and sizes. The conspicuous success of Carman's method provided the incentive for the present research, since the lack of dependence on the shape of the particles concerned suggested its application to fibrous materials.

The investigations to be described consist largely of the verification of the Kozeny equation for particles approximating true fibrous materials in their physical form. The materials employed were selected by virtue of their susceptibility to actual measurement of specific surface for purposes of comparison with calculated values. Various liquids are used as the "measuring fluids" for the work discussed in section Ia, while in section Ib, the Carman method is extended to include the use of gases. Comparisons are made between liquid and gas permeability results, since

comparative values should reflect any fundamental differences in the factors involved in liquid and gas flow.

It seems appropriate at this point to insert a few words of explanation regarding the incomplete nature of certain phases of the investigation. The results obtained up to the time of outbreak of hostilities were so encouraging that it was deemed advantageous to apply them immediately to certain problems of national importance. As a result, many other matters of considerable academic (and practical) interest were neglected. Outstanding deficiencies are a more rigorous comparison of permeability values obtained with various liquids and gases, and a systematic investigation of the effects of fibre orientation and uniformity of packing. It is hoped that this apparent oversight will be pardoned in view of the unusual situation.

As a background for the work to be described, a brief survey of the general field of surface area determination will be presented. A more extended discussion of the theoretical foundations and development of the Kozeny-Carman method is given, an acquaintance with these subjects being desirable for interpretation of the experimental results.

#### HISTORICAL REVIEW AND INTRODUCTION

Within recent years many workers have devoted themselves to the study of fine particles, principally within the range O.l micron to O.l cm. Methods of determining particle size and size-distribution curves for a powder sample have been brought to a high degree of perfection, if not of simplicity. Owing to the availability of such data, the size of particles has been used to obtain an approximate measure of their surface area. The most generally accepted procedure is that of Heywood (5), which has been advocated by the Institution of Mechanical Engineers. In brief outline, this method of calculation involves the following steps:-

evaluated by elutriation or sieve analysis, according to the range covered. For liquid sedimentation, the photo-electric turbidimeter of Wagner (6) and the pipette sampling method of Andreasen (7) are in most common use. Liquid sedimentation is acceptable for particles above an approximate lower limit of 5 \mu if proper dispersion of the powder is obtained. Below this size convection currents usually introduce serious error, although the photographic sedimentation methods of Carey and Stairmand (8) have been applied to particles as small as 1 \mu . Air elutriation has been used by Roller (9)

but while accurate for particles of 5 M diameter, is very slow.

(b) Representative particles from a convenient size fraction are examined microscopically: the projected areas and perimeters of the particles are measured while resting in their most stable positions on the microscope slide. By counting and weighing the selected particles the average particle weight may be calculated, and therefore also the average volume (the density being known).

To utilize these measurements, Heywood has developed an equation from first principles which enables the surface area to be calculated without making any simplifying assumptions regarding particle shape. A "shape factor" relating surface area and particle dimensions is obtained from the microscopic examination data, thus giving the specific surface (area per unit volume) for the one size fraction.

It is finally assumed that the average particle shape (and hence the shape factor) is independent of size, so that the total average specific surface may be calculated from the size-distribution curve for the powder.

Although widely used for fine powders, the Heywood method suffers seriously from tediousness. Further, the values obtained may be little more than approximations, since the assumption that shape is independent of size is not always justified. In any event, this approach is totally

unsuited to the complex forms found in fibrous materials.

A variety of other methods has been developed which are useful in certain cases, but are seldom widely applicable or capable of a very high degree of accuracy.

The rate of dissolution in a suitable corrosive medium has been employed by first determining the rate of solution per unit area of a solid piece of the material.

The surface area of the finely divided material is then calculated by simple proportion. This method has been applied successfully by Marten (10) to ground quartz, using hydrofluoric acid as solvent. However, at least two serious objections exist. In a material containing a range of sizes the smallest particles may disappear entirely during solution; further, it is extremely doubtful whether the boundary conditions governing the rate of solution are identical for all sizes of particles.

The turbidity of a suspension of fine particles in a suitable liquid yields a measure of their surface area, since for sizes which are large with respect to the wavelength of light, reflection is the principle factor and turbidity is directly proportional to area. The turbidity of the suspension may be measured most conveniently by means of the "turbidimeter" which compares the intensity of light transmitted through a given depth of suspension with that transmitted by a similar depth of liquid containing no suspended

solids. The calculation of surface area from turbidimeter data is discussed in detail by Munro (11), and applied to powdered alundum, transparent and opaque silica, and wood pulp fibres.

Still another method is based on measurement of the adsorption of a suitable substance on the surface. Various dyes have been employed by Tunstall (12), and argon at liquid air temperature by Askey and Feachem (13). The latter undoubtedly gives a measure of the total surface area, but includes all internal fissures and voids in addition to the overall external surface.

Fortunately, the new approach to the problem of surface area determination, developed by Carman on the basis of Kozeny's relation, suffers from almost none of the usual disadvantages. A preliminary determination of the size distribution curve for the material is not required, resulting in a great saving of time. Even more important is the absence, theoretically at least, of limitations as to size or shape of the particles constituting the material. To elucidate this point, it seems desirable to present a fairly complete account of the fundamental principles underlying the fluid permeability method.

The basic physical principles governing the flow of fluids through a porous medium (such as a bed of fine

particles) must, in general, be identical with those operating in the case of viscous flow in any other type of system; i.e. those expressed in the Stokes-Navier equations of classical hydrodynamics. Unfortunately, however, the rigorous solution of hydrodynamical equations for all the boundary conditions existing, for example, in an ordinary sand bed would be hopelessly complex. It was only to be expected that the first approaches were by way of purely experimental study.

The now classic experiments of Darcy (14) led to the very simple generalization that the rate of flow (Q) of a homogeneous fluid through a porous medium may be described as follows:

Q is directly proportional to the cross-sectional area (A) of the medium, inversely proportional to its length (L), directly proportional to the difference of fluid head ( $\triangle$ h) between inlet and outlet, and inversely proportional to the kinematic viscosity ( $\nu$ ) of the fluid. The preceding relations may be combined to give the following equation, commonly termed "Darcy's Law":-

$$Q = C \frac{A \triangle h}{\nu L}$$
 (1)

C is a proportionality constant, characteristic of the medium.

This equation has been shown to be valid for all types of porous media - collodion membranes (15), filter cakes (16), rorous plates (17), sands (18) and fine powders (19). While equation (1) is of very simple form, and would be anticipated by analogy with Poiseuille's law, no satisfactory general analytical justification for its existence has yet been presented (20). Only in the case to be discussed, i.e. beds of unconsolidated particles, has it been possible to develop an adequate theoretical foundation.

The applicability of Darcy's law is confined to the region of "streamline" flow. By the method of dimensional analysis, the following general equation may be developed for flow rates in any system:

$$\frac{\Delta p}{\Delta x} = \text{const.} \frac{\mu^2}{\rho d^3} f(\frac{dv\rho}{\mu}) \qquad (2)$$

Where  $\triangle p$  = pressure drop in system over a length  $\triangle x$ . i.e.  $\triangle_{\triangle x}^{\triangleright}$  = pressure gradient producing the flow.

v = average velocity of flow

 $\rho$  = density of fluid

d is a linear dimension; its implication depends on the type of system concerned. It may characterize the size of pore openings, tube diameters, etc.

When applied to ordinary pipe flow, the term  $(\frac{d\mathbf{v}\rho}{\mu})$  is termed the "Reynolds number" = R. For low values of R, the function  $f(\mathbf{R})$  of equation (2) is found to simply equal R.

Hence, 
$$\triangle p / \triangle x = const. \frac{\mu v}{d^2}$$
 (3)

The above result is identical with Poiseuille's law. This type of flow is termed "streamline", the velocity components being essentially parallel to the enclosing walls.

As the Reynolds number is increased, for example by increasing "v", a critical value is reached at which the type of flow changes quite abruptly from "streamline" to "turbulent". Turbulent flow is found to be characterized by a new value for f(R), which then is equal to  $R^2$ .

Thus 
$$\triangle p / \triangle x = const. \frac{p v^2}{d}$$
 (4)

In the case of porous media, the transition from streamline to turbulent flow is not sharp; this result is logical from consideration of the variety of pore diameters in such a medium, since with increasing velocity turbulent flow will be introduced in more and more channels. For convenience, the term "streamline flow" as applied to a porous medium is defined as the region in which Darcy's law applies, i.e.  $\Delta p/\Delta x \propto v$ . A method of calculating the approximate threshold value beyond which increased flow velocities result

in appreciable deviations from Darcy's law will be given in a subsequent section. It should be noted that the paralleliam between pipe flow and overall flow through a porous medium must be treated with caution, since fundamental differences exist. For example, in a single tube of circular cross-section the velocity distribution curve taken across the section is parabolic under conditions of streamline flow, having a maximum value at the centre and falling to zero at the walls. For a uniform porous medium, however, the macroscopic velocity is constant over the cross section since it is the average of a large number of individual channel velocities. As a consequence, the total flow in unit time for a single tube is proportional to d<sup>4</sup>, i.e. to A<sup>2</sup>, (eq'n. 3) but for a linear porous medium is proportional to A.

At very low velocities Darcy's law again becomes invalid, the pressure gradient required being greater than that expected for the particular flow rate. It has been suggested by Carman (3) that an abnormally thick stationary layer of fluid remains in contact with the surfaces of the constituent particles of the bed, resulting in decreased free volume of the channels and hence decreased flow rates. For velocities within the ordinary range this stationary layer may be largely removed. Evidence for the existence of such

stagnant layers has been provided by several investigators.

This phenomenon will be discussed more fully in Section Ib, since it is of importance in fixing a lower limit of applicability of the permeability method.

For the condition of streamline flow, it has already been shown that  $f(\frac{dv\rho}{\mu}) = \frac{dv\rho}{\mu}$ 

Hence equation (2) may be written

$$v = const. \frac{d^2}{\mu} (\frac{dp}{dx})$$
 (5)

This equation may be used to extend the application of Darcy's law to the general problem of linear flow of homogeneous fluids through porous media. (21). For such a case, d will represent the effective diameter of the stream channels in the medium, while v = macroscopic velocity of the fluid. As before, dp/dx is the (macroscopic) pressure gradient. The proportionality constant is a true constant dependent only on the geometric properties of the medium.

A general expression evaluating the constant in terms of the geometrical characteristics of the medium would be very desirable, as it would enable calculation of physical dimensions of the medium from flow data, or the converse. As a result, several investigators (22,23) have attempted to derive theoretical relations embracing the various quantities involved.

While a literal solution of the problem is obviously well-nigh

impossible, Kozeny (1,2) has proposed certain simplifying postulates which enable a reasonable solution to be made.

Kozeny assumes that the pore space of a bed of unconsolidated particles may be considered as equivalent to a group of parallel, similar channels, such that the total internal surface and volume are respectively equal to the total particle surface area and pore volume.

Then let E = volume of pore space open to the fluid per unit volume of bed, i.e. fractional free volume or "porosity"

S = total surface area of particles per unit volume of bed.

Dupuit (24) has postulated that if the pore space be considered as uniformly distributed throughout the bed, the porosity of a thin layer normal to the direction of flow will be identical with the porosity (£) of the bed as a whole. Then for such a layer the fractional free volume will also express the fractional free area of cross-section.

Kozeny employs Dupuit's assumption to estimate the interstitial velocity. If u = macroscopic linear velocity of the fluid, the component of the average interstitial velocity parallel to the macroscopic flow direction will be u. However, the actual path followed by an element of fluid will be sinuous, and hence of total length L. (which

is always greater than the depth of bed L). Since the time required for the fluid to traverse a path of apparent length L at a velocity of u/E is identical with that required for a path of length Le at the true interstitial velocity ue,

$$u_e = \frac{u}{E} \cdot \frac{L_e}{L}$$
 (6)

It has been shown by hydrodynamical analysis that the average velocity of flow of a viscous fluid through linear channels with cross-sections of various shapes does not change greatly as the shape is varied, if the results be expressed in terms of the ratio of cross-sectional area to "wetted perimeter". (25). This last term  $\frac{A}{P_W}$  is also equivalent to the ratio of the volume of the channel to the area exposed to the fluid.

The average velocity of a viscous fluid moving in a channel of constant cross-section under conditions of stream-line flow may be expressed by

$$\frac{1}{\mathbf{v_r}} = \frac{\mathbf{k'}}{\mu} \left( -\frac{\mathbf{dp}}{\mathbf{dr}} \right) \left( \frac{\mathbf{v}}{\mathbf{s}} \right)^2 \tag{7}$$

Where  $\overline{V_r}$  = velocity in the flow direction r

dp/dr = pressure gradient along channel producing the flow

V = volume of channel

s = area exposed to fluid

k = a dimensionless shape factor.

As stated above, the factor k' does not vary widely with change of shape of channel cross-section. Typical values are given in Table I.

#### Table I.

Shape Factor k' for Various Channel Cross-Sections (3)

Shape of cr	oss-section	<u>k'</u>
Circular Elliptical	major axis = 2 times minor major axis = 10times minor	0.500 0.476 0.414
Rectangular		0.562 0.515
n ñ	" =10 " "	0.377
7	$ \begin{array}{cccc}  & & & & & & & & & \\  & & & & & & & & \\  & & & &$	0.333
Equilateral		0.600

Equation (7) may be applied to the entire bed by replacing the ratio  $\frac{V}{s}$  by  $\frac{E}{S}$ , -dp/dr by  $\frac{\Delta p}{L_e}$  (where  $\Delta p$  = total pressure drop across the bed) and  $\frac{\Delta p}{V_r}$  by  $u_e$ .

Then 
$$u_e = \frac{u}{\varepsilon} \cdot \frac{L_e}{L} = \frac{k'}{\mu} \cdot \frac{\Delta p}{L_e} \cdot \frac{\varepsilon^2}{S^2}$$
  
and  $u = k' \frac{L}{L_e} \cdot \frac{\Delta p}{\mu} \cdot \frac{\varepsilon^3}{S^2}$ 

Setting  $k = k' \left(\frac{L}{Le}\right)^2$ , the following expression results:- $u = \frac{k}{\mu} \cdot \frac{\Delta p}{L} \cdot \frac{\epsilon^3}{S^2}$  (8)

Consistent units should be used throughout, i.e. if the C.G.S. system be employed,  $\triangle$  p is expressed in dynes/cm.<sup>2</sup>.

Equation (8) has come to be known as the "Kozeny equation". With the exception of the constant k, all the factors in the equation may be measured directly as physical properties of the medium. The theoretical reasoning presented above allows prediction of the order of magnitude of k, while an accurate value may be determined by experiment.

Bartell and Osterhof (26) obtain an approximation to k by assuming that the "equivalent channels" may be circular, for which k' = 0.500. Combined with Hitchcock's assumption (27) that  $\frac{L}{L_0} = \frac{2}{\pi}$ , the resulting value for k is then

$$k = 0.5(\frac{2}{\pi})^2 = 0.20$$

However, Carman has found experimentally (3) that with spheres the average direction of flow is inclined  $45^\circ$  to the axis of the bed, thus indicating that  $\frac{L}{L_0} = \frac{1}{\sqrt{2}}$ . Carman considers this to be a more probable value for materials approaching spherical form, yielding a value of

$$k = \frac{0.5}{2} = 0.25$$

As a result of experimental work with the flow of

ground waters through sand beds, Kozeny (2) obtained a value of about 0.3 for k. Analysis of a great variety of data from his own investigations together with those of other workers led Carman to assign a value of 0.20 to k. Recent reports by Fowler and Hertel (28) and Sullivan and Hertel (29), published after the completion of the research to be described, indicate values of k = 0.18 for fibrous materials and k = 0.222  $\pm$  .001 for uniform glass spheres.

A slightly different derivation of the Kozeny equation enables more light to be cast on the theoretical significance of k. The deductions given follow those presented in the paper of Fowler and Hertel (28):-

Equation (7) will be valid for a short section of a passage in a porous medium, giving the flow velocity in the direction of the passage. Let the angle between this direction and the X axis (the long axis of the medium as a whole) be termed 9. Then the velocity component in the X direction will be

$$\frac{1}{\nabla_{x}} = \frac{k!}{\wedge} \left(-\frac{dp}{dr}\right) \left(\frac{\nabla}{s}\right)^{2} \cos \theta \tag{9}$$

If \_\_ be averaged over the entire free space of  $v_x$  the medium, the final result may be expressed in the form

$$\left\langle \frac{\mathbf{v}_{\mathbf{x}}}{\mathbf{v}_{\mathbf{x}}} \right\rangle_{A\mathbf{v}} = \frac{\mathbf{k}}{\mu} \left( -\frac{\delta p}{\delta \mathbf{x}} \right) \left\langle \frac{\mathbf{v}}{\mathbf{s}} \right\rangle_{A\mathbf{v}}^{2} \tag{10}$$

where  $\delta p/\delta x$  is the macroscopic pressure gradient for the medium.

In this summation, two cases may be distinguished. If the flow channels be regarded as bundles of more or less independent tubes, transverse pressure gradients will not influence the system; the same total flux will be found in all sections of any one channel regardless of its orientation. For this first case, dp/dr must fulfil the above condition, and must be independent of 9.

Expressing &p as a line integral:

$$\delta p = \int \frac{dp}{dr} \cdot dr = \left\langle \frac{dp}{dr} \right\rangle_{AV} \int \sec \theta dx$$

$$= \left\langle \frac{dp}{dr} \right\rangle_{AV} \left\langle \sec \theta \right\rangle_{AV} \delta x \qquad (11)$$

Then from (9), (10) and (11)

$$k = k' \left\langle \frac{\cos \theta}{\sec \theta} \right\rangle_{Av}$$
 (12)

A second case is possible, in which the system cannot sustain transverse pressure gradients without disturbance. For this condition, dp/dx is independent of the orientation and hence of  $\theta$ . It may then be shown that

$$\frac{dp}{dr} \cos \theta = \frac{dp}{dx} \cos^2 \theta$$

and

$$k = k' \left\langle \cos^2 \theta \right\rangle_{Av} \tag{13}$$

Thus 
$$\frac{k}{k}$$
, may have values of  $\frac{\langle \cos \theta \rangle_{AV}}{\langle \sec \theta \rangle_{aV}}$  or

 $\left\langle\cos^2\theta\right\rangle_{AV}$  , according to the initial assumption selected.

If Q = volume of fluid entering the bed of uniform cross-sectional area A per unit time, the macroscopic velocity of the fluid = Q/A. The average X-component of the microscopic pore velocity will then be  $Q/A\epsilon$ .

Let there be N particles of average volume T per unit volume of the medium; then N.T= (1-E), or N =  $\frac{1-E}{m}$ .

If the average area of each particle =  $\sigma$ , the total area of the particles in each unit volume of medium

$$= N\sigma = \frac{(1-\varepsilon)}{T}\sigma$$

Since & = free space per unit volume of medium, the volume of free space associated with unit surface area will be given by

$$\frac{\mathcal{E}}{\left[\frac{(1-\mathcal{E})\sigma}{T}\right]}$$

If, in equation (10), the average square of the free space per unit area be approximated by the square of the average free space per unit area, the expression becomes

$$\frac{Q}{A} = \frac{k}{\mu} \cdot \frac{g^3}{(1-g)^2} \left(\frac{T}{\sigma}\right)^2 \left(-\frac{\delta p}{\delta x}\right) \tag{15}$$

Equation (15) is identical with equation (8) previously obtained, since

$$\frac{Q}{A} = u$$
,  $-\frac{\delta p}{\delta x} = \frac{\Delta p}{L}$ , and  $\frac{(1-E)\sigma}{T} = S$ .

The fluid will, in general, move in directions parallel to the boundaries of the channels; hence a theoretical estimation of k may be made by assuming that all orientations of the channels are equally probable. On this basis,

$$\langle \cos \theta \rangle = \frac{\pi}{4}$$
,  $\langle \cos^2 \theta \rangle_{AV} = \frac{2}{3}$ ,  $\langle \sec \theta \rangle_{AV} = \frac{\pi}{2}$ 

and hence k is either  $\frac{1}{2}$  k' or 2/3 k' depending on whether dp/dr or dp/dx is considered to be independent of the orientation. Conversely, accepting the approximate value of k = 0.2,  $\langle k' \rangle_{AV}$  would be 0.4 or 0.3 respectively. Comparison with the values of the shape factor k' given in Table I. indicates that the stream channels of the medium possess quite elongated cross-sections, which is in accord

with expectation.

Carman (4) has expressed equation (8) in a form which is slightly more convenient for purposes of calculation by introducing a new term, the permeability. The permeability (K) of a porous medium is defined as the linear rate of fluid flow produced by unit hydraulic gradient. For a given fluid viscosity and density, K measures a specific property of the bed. K has the dimensions of a linear velocity, and by definition

For a liquid flowing under its own head,

$$K = \frac{Q}{A} \cdot \frac{L}{b} \tag{16}$$

where h = head of liquid (cm.) producing the flow

L = depth of bed (cm.)

Q = total flow (cm. 3 /sec.)

A = area of cross-section of bed (cm.<sup>2</sup>)

Rewriting equation (8),  $\frac{Q}{A} = \frac{k}{\mu} \cdot \frac{h \rho g}{L} \cdot \frac{g^3}{S^2}$ , since  $\Delta p = h \rho g$  where  $\rho$  = density of liquid (gm./cm.<sup>3</sup>)

 $g \approx 980 \text{ cm./sec.}^2$ 

If the "specific surface" ( $S_o$ ) of the constituent particles be defined as the surface area per unit volume of solid material in the bed, then  $S = S_o(1-E)$ . (S= surface area/unit volume of bed).

Further substituting  $\upsilon$  (kinematic viscosity of the liquid) for  $\mu/\rho$  ,

or 
$$S_{0} = \frac{kq}{\nu} \cdot \frac{1}{S_{0}^{2}} \cdot \frac{E^{3}}{(1-E)^{2}}$$

Using k = 0.20 and g = 980 cm./sec.<sup>2</sup>, equation (17) becomes

$$s_0 = 14\sqrt{\frac{1}{K\nu} \cdot \frac{E^3}{(1-E)^2}}$$
 (18)

Equation (18) may conveniently be used for calculation of the specific surface of the constituent particles of a filter bed. The permeability of the bed is first obtained from the rate of flow of some suitable fluid through the bed under a given head. (equation 16). The porosity £ is simply the ratio of the volume of the constituent particles to the total volume of the bed, the former quantity being determined from the weight and density of the material. All required factors are then known.

Carman (3.4) undertook a systematic investigation of the applicability of equation (18), for a wide variety of conditions. By variation of each of the physical characteristics of the bed over a considerable range, it was possible to show whether the factors included in the equation expressed these variables in correct relation. In equation (18), the fundamental variables to be checked were the kinematic viscosity of the fluid. the porosity of the bed, and the specific surface of the material. It was also necessary to show that the experimental results were independent of factors not appearing in the equation. i.e. the shape of the particles and the presence of size ranges.

A study was first made of the effect on the permeability of the bed when So was varied, by employing particles of various sizes but of identical shape. For this purpose use was made of Schriever's data (30) for glass spheres. covering a range in diameter of 0.025 to 0.1025 cm. found that the factor

$$\frac{K}{d^2} \cdot \frac{(1-E)^2}{E^3}$$

was constant within ± 3% for all sizes, demonstrating that  $K \propto d^2$  as predicted by the Kozeny equation; also that the term (1-E)<sup>2</sup>

gave at least the right order of correction for the inevitable porosity variations between beds formed of spheres of different diameters.

The kinematic viscosity factor v was then tested by the flow of nine different liquids through a bed of sand composed of particles in the range 0.014 to 0.021 cm. The liquids used ranged from diethyl ether (v = .00342) to aniline (v = .0478); air (v = 0.157) was also employed. The factor

$$K \mathcal{D} \frac{(1-\epsilon)^2}{\epsilon^3}$$

was found to be constant within  $\pm$  3%, indicating that  $k \propto \frac{1}{\nu}$  as required.

The porosity function  $\frac{\mathcal{E}^3}{(1-\mathcal{E})^2}$  represents probably the most important factor in the Kozeny equation, since a small variation of  $\mathcal{E}$  produces a very large change in the value of the function as a whole (31). By collection of the data of other workers on silica powder (19), flaky flint sand (32), slate powder (19), together with permeability experiments for short lengths of crimped wire, small Berl saddles and Lessing rings, Carman was able to cover a porosity range of 0.260 to 0.889. This corresponded to more than a thousand-fold variation of the porosity function. While no comparison between different materials was possible, a

constancy of  $\pm$  2% for calculated values of S<sub>0</sub> was found over the range of porosities obtainable with each sample.

The development of the Kozeny equation suggested no limitations as to the shape of the particles comprising the porous medium, so that it was to be expected that the general form of the equation would be the same in all cases. However, it was not at all certain that the proportionality constant would be invariant. Since his original assignment of the value k = 0.20 resulted from analysis of data for near-spherical particles only, Carman next investigated beds composed of units departing considerably from spherical form. For this purpose 0.6 cm. nickel Lessing rings, 0.6 cm. porcelain Berl saddles, and 0.57 cm. lengths of .03 cm. diameter crimped steel wire were selected. In each case the specific surfaces calculated from the geometry of the units and from the Kozeny equation using the value k = 0.20, were in agreement within ± 2%. This error was in the order of the accuracy of the measurements.

Investigations were made regarding a further point on which no information was given by the theoretical reasoning, namely, the validity of the calculations when a range of sizes were present in the bed of particles. The data of Coulson (33) for mixtures of steel spheres of 1/16" to 5/16" diameter yielded calculated values of average specific

surface in close agreement with the true values. Extending this range, Carman (4) used mixtures of two sands, of approximately .01 and .05 cm. average particle diameter, containing from 5% to 40% of the smaller size; mixtures of two sands each of .05 cm. average particle size but of different grain shapes were also employed. In all cases agreement within ± 2% was found between the values of So calculated (a) from the permeability of the bed, and (b) from the relative amounts of each sand present, the specific surface of each sand being itself calculated from permeability determinations.

Measurement of the permeability of a material necessarily involves the use of a container for the bed, so that some type of correction for wall friction is required. Considering a bed enclosed in a cylindrical tube of diameter D cm., the wall surface per unit volume of bed is 4/D, and as a first approximation S might be replaced by  $S+\frac{4}{D}$ . However, Carman has found experimentally that  $S+\frac{2}{D}$  is more nearly the required value; probably  $S+\frac{4}{D}$  is excessive since the entire wall surface is parallel to the macroscopic flow direction. The experiments of Coulson (33) with spheres of 0.16 to 0.8 cm. diameter in a containing tube of 5.08 cm. diameter substantiate Carman's factor  $\frac{2}{D}$ .

Replacing S by  $(S + \frac{2}{D})$ , and recalling that S = Sd(1-E), equation (18) becomes

$$S_0 = 14\sqrt{\frac{1}{K\nu} \cdot \frac{E^3}{(1-E)^2}} - \frac{2}{D(1-E)}$$
 (19)

Thus the specific surface may be calculated as usual and then corrected for wall friction by subtracting the term  $\frac{2}{D(1-E)}$  .

The magnitude of the wall correction is illustrated by data obtained by Carman for glass spheres of 0.472 cm. diameter:

$\overline{\mathtt{D}}$	So (uncorrected)	Wall correction
5.01 cm. 2.39 " 1.38 "	13.4 cm. <sup>2</sup> /cm. <sup>3</sup> 14.2 15.0	0.7 cm. <sup>2</sup> /cm. <sup>3</sup> 1.5 2.6

As indicated by equation (19), the relative importance of the wall correction diminishes as the container diameter and/or the specific surface of the material are increased. In almost all of the experiments to be described in the following sections the values of specific surface are so large that the term  $\frac{2}{D(1-E)}$  may be neglected without introducing appreciable error.

It should be mentioned that, in addition to the Kozeny equation, other and slightly different equations have been proposed to relate specific surface and permeability for a bed of unconsolidated particles. Those of Burke and Plummer (34) and Chilton and Colburn (35) have been deduced from a combination of dimensional analysis and experimental data. The Chilton and Colburn equation reduces to the Burke and Plummer equation for the case of spherical particles. Expressing Burke and Plummer's relation in the notation used by Carman.

$$S_0 = 14.1 \sqrt{\frac{1}{K^2} \cdot \frac{E^2}{(1-E)}}$$
 (20)

This is equivalent to the Kozeny equation only for the condition & = 0.5, and does not agree with the considerable accumulation of experimental evidence for other values of the porosity. Actually, values of porosity in the order of 0.5 obtained in the experiments performed by the above authors.

Carman's extensive investigations indicated that the Kozeny equation might be applied with confidence to materials in the range covered by the experiments. However, the greatest departure from spherical form was represented by the wire crimps, with a ratio of length to diameter of

approximately 20. Before attempting to apply the permeability method to actual fibrous materials, it was necessary to extend the study to particles of smaller diameter and much greater ratio of length to effective diameter. This phase of the investigation forms the subject matter of Part 3 of this section.

#### EXPERIMENTAL PROCEDURE AND RESULTS

### (a) Equipment and General Procedure

The apparatus employed for the measurement of liquid permeability is shown in Figure 1.

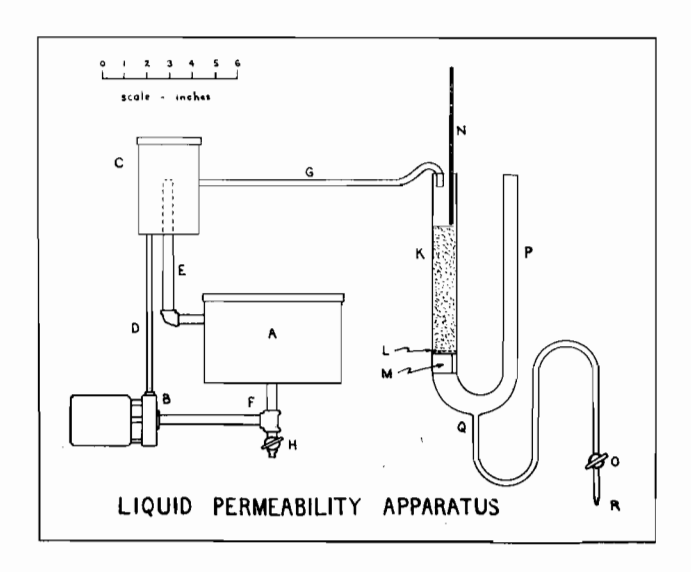


Figure 1.

A liquid reservoir A of approximately 2 liters capacity is connected through a midget centrifugal pump B to an overflow type constant level device C. This portion of the apparatus serves to maintain a steady supply of liquid to the permeability measuring tube at constant head. The assembly is constructed entirely of metal and is mounted as a unit to allow ready adjustment to any desired height.

The pump is a Fisher Model A monel metal midget circulating pump with a rated capacity of 5 gallons per minute.

Since only a small fraction of this delivery is ever required the outlet is throttled by using a 1/16 inch bore copper tube at D. The return lines E and F are standard 1/4 inch brass pipe, while the delivery tube G is 3/16 inch copper tubing. Loose covers are fitted to reservoirs A and C to retard evaporation of volatile liquids. A small plug cock H is included to facilitate drainage of the apparatus before changing to a different liquid.

The permeability measuring tube shown at the right hand portion of Figure 1 is similar to that employed by Carman (4). The tube is constructed of Pyrex glass. The bed of material to be investigated is packed into the left hand limb K, resting on a circle of copper gauze L. The circle of gauze is carefully cut to fit the tube and is supported by a flat-wound spiral of sheet brass M. The mesh size of the gauze is selected for each material so that the smallest particles may be retained, but so that the resistance to flow offered by the gauze is negligible in comparison with that of the bed.

A constant head of liquid is maintained in the permeability measuring tube by means of the circulating pump and overflow system described above. The temperature of the incoming liquid is measured by the thermometer N. The rate of flow of liquid through the bed of material is controlled by the stopcock O, and the resulting head loss is indicated by the difference between the liquid levels in limbs K and P.

The pressure drop measured in this way is actually that due to all frictional and expansion losses between the liquid surface in K and point Q, but for practical purposes may be assumed to be due to the resistance of the bed alone. The liquid level in limb P is read on a mirror scale graduated in 1 millimeter divisions, mounted behind the tube. This scale is also used to measure the liquid level in limb K and the depth of the bed of material; these readings being transferred to the scale by means of an index line on a ver-The rate of flow is measured tically-adjustable cursor. by weighing the liquid emerging from R in a definite time For volatile liquids and very low flow rates, precautions must be taken against loss by evaporation. majority of cases, negligible loss occurs if the jet R extends well into the neck of a narrow-mouthed weighing bottle. high flow rates and non-volatile liquids, speed of operation may be gained by the use of a tilting glass trough arranged to direct the flow from one beaker to another at predetermined times.

The permeability measuring tubes were constructed with various lengths and diameters for limb K, depending upon the permeability of the material and the viscosity of the liquid to be used. The glass tubing for limb K was carefully selected for uniformity of cross section. After construction the tube was calibrated by filling limbs K and P with water, closing

the mouth of P, and weighing the water run out for a series of levels in K.

The most important, and frequently the most difficult portion of the procedure was the production of a uniform, air-free bed of solids. The bed was most conveniently prepared by partially filling the permeability measuring tube with the desired liquid, then introducing a definite weight of the solid material with constant stirring. In addition, it was frequently necessary to close limb P and apply suction at K to complete the removal of entrained air. This latter procedure was invariably required with materials of fibrous form.

Due to the manipulative difficulties which would have resulted, the apparatus was not enclosed in a constant-temperature bath. Satisfactory results were obtained by mounting the apparatus in a portion of the laboratory which was sheltered from draughts. The temperature indicated by thermometer N showed few erratic changes; the effect usually encountered was a slow rise in temperature due to heating of the liquid by the circulating pump.

The densities and viscosities of the liquids employed in the investigation were taken from the International Critical Tables. The densities of the solid materials were measured by displacement of benzene or water in a pyknometer flask.

The experimental results obtained with the liquid

permeability apparatus were used for calculation of specific surface by means of the Kozeny-Carman relation, equation (18):

$$S_0 = 14\sqrt{\frac{1}{K\nu} \cdot \frac{\varepsilon^3}{(1-\varepsilon)^3}}$$

Where  $S_0$  = specific surface of solid material (sq. cm./cc.)

K = permeability of bed (cm.)

 $\mathcal{E}$  = porosity of bed

v = kinematic viscosity of liquid (sq. cm./sec.)

A sample calculation is shown in the following section.

## (b) Measurements with Screen-Classified Sand

The first measurements were made with beds of screen-classified sand to obtain familiarity with the procedures involved and to check Kozeny's relation for particles of simple form.

A quantity of clean sand was separated into the fractions of the Tyler standard screen scale using a mechanical sifter. Each fraction was then washed with water in a simple elutriation device to remove very fine particles. The average density of the sand grains of each fraction was measured by displacement of water in a pyknometer flask. The permeabilities of sand beds to water were determined for size fractions ranging from 10 mesh to 65 mesh. In addition, the permeabilities to benzene were determined for the fractions 28 to 35 mesh and 35 to 48 mesh. The experimental results obtained

in a typical determination were as follows:

Size fraction = 20 to 28 mesh (.0833 to .0589 cm.)

Liquid employed = distilled water

Weight of sand = 73.5 grams

Average density of sand = 2.67 grams

Depth of bed (L) = 9.71 cm.

Diameter of bed (D) = 2.515 cm.

Cross-sectional area of bed (A) = 4.97 sq. cm.

Permeability  $K = \frac{QL}{Ah} = \frac{\text{flow rate (cc./sec.)}}{\text{area of bed (sq.cm.)}} \frac{\text{depth of bed (cm.)}}{\text{head loss (cm.)}}$ 

The values of KD in Table II show a deviation of ±2 1/2% from the mean. This range is slightly greater than that to be expected from the experimental error. It may be noted from Table III that the values of KD show an irregular but significant decrease when listed in order of increasing flow rate. Since the runs were not performed in this order, the effect cannot be attributed to changing temperature, separation of air within the bed, or other factors dependent on elapsed time.

A calculation of the true specific surface of the sand bed was made from the geometry of the constituent particles to allow comparison with the value obtained by the permeability method. However, serious uncertainties were introduced by the wide variation of shapes of the constituent particles and by the fact that the relative proportions of the

TABLE II Permeability Measurements with 20 to 28 Mesh Sand.

Run	Head Loss h	Flow Rate Q	Water Temperature	Kinematic Viscosity $\nu$	Permeability K	Kυ
123456789011	5.88 cm. 5.96 5.84 9.13 9.11 9.23 12.48 12.48 17.67	1.303 cc./sec. 1.336 1.325 2.029 1.997 2.039 2.695 2.695 2.700 1.669 2.330	21.2°C 21.3 21.5 21.5 21.5 21.7 21.7 21.7 21.7	980x10 <sup>-5</sup> sq. em./sec. 978 974 974 974 972 970 970 970 968 968	0.434 .438 .444 .434 .428 .432 .422 .424 .422 .427	4.25x10 <sup>-3</sup> 4.29 4.32 4.22 4.18 4.20 4.12 4.10 4.12 4.10 4.13
				A·	verage Kv=	4.19x10-3

Volume of bed =  $9.71 \times 4.97 \text{ cc.} = 48.3 \text{ cc.}$ Actual volume of sand =  $\frac{73.5}{2.67}$  cc.= 27.5 cc.

Free volume =  $\frac{20.8 \text{ cc.}}{}$ 

Porosity 
$$\varepsilon = \frac{20.8}{48.3} = 0.430$$

Calculated specific surface So =  $14\sqrt{\frac{1}{K\nu} \cdot \frac{\xi^3}{(1-\xi)^2}}$ 

Correction for wall surface =  $\frac{2}{D(1-\epsilon)} = 1.4 \text{ sq. cm./cc.}$ 

Corrected specific surface = 116.8 - 1.4 = 115.4 sq. cm./cc.

Flow Rate Q	Kυ	Flow Rate Q	Kυ
1.303 cc./sec.	4.25x10 <sup>-3</sup>	2.039 cc./sec.	4.20x10 <sup>-3</sup>
1.325	4.32	2.330	4.13
1.336	4.29	2.695	4.12
1.669	4.20	2.695	4.10
1.997	4.18	2.700	4.12
2.029	4.22		

various shapes were not constant over a range of sizes. The best estimates which could be made indicated that the true specific surface lay in the range  $\frac{6}{d_1}$  to  $\frac{g}{d_1}$ , where  $d_1$  was taken as the average of the minimum diameters of the sand grains examined. The true surface for the fraction 20 to 28 mesh was thus 90 to 120 sq. cm./cc.

The results from the complete series of measurements with sand beds are summarized in Table IV. The product of the specific surface and the average particle diameter (actually the average mesh opening) is listed for each size fraction in the last column of the table. If the shape of the sand grains were constant for each fraction, the product Sod should also be constant. The variation actually found is of the same order and in the same direction as that predicted from microscopic examination of the constituent particles.

The specific surfaces of the 28 to 35 mesh and 35 to 48 mesh fractions obtained by measurement of the permeabilities to benzene were in both cases lower than those obtained by the use of water. The differences were 2 1/2% and 9% respectively.

Table IV also illustrates the relative magnitude of the wall correction for particles of various sizes. The wall correction in this instance became less than the experimental error for particles smaller than 35 mesh.

TABLE IV

Permeability measurements with Screen-Classified Sand

Size Fraction mesh	Average Particle Diameter cm.		orosity	Specific Surface (uncorrected) sq.cm./cc.	Wall Correction sq.cm./cc.	Specific Surface (corrected) sq.cm./cc.	S₀₫
10 to 14	0.141	Water 1.163x10-2	0.440	67.9	1.4	66.5	9.38
20 to 28	.0711	Water 4.19x10-3	.430	116.8	1.4	115.4	8.20
28 to 35	.0503	Water 2.15x10-3	.443	160.8	1.4	159.4	8.02
28 to 35	.0503 B	Benzene 2.58x10-3	.456	157.0	1.5	155.5	7.83
35 to 48	.0356	Water 9.28x10-4	.436	235	1.4	234	8.33
35 to 48	.0356 в	enzene 1.267x10-3	.447	21.3	1.4	21.2	7-55
48 to 65	.0252	Water 5.61x10-4	.430	293	1.4	292	7.36

## (c) Measurements with Small Glass Rods

The first step toward the investigation of elongated particles was taken by the use of short lengths of slender glass rod. This material was prepared by drawing out heated glass rod to an approximate diameter of 0.04 centimeters, rejecting oversize and undersize portions, and cutting into 8 millimeter lengths. The diameters of a random sample of 200 of these rods were measured with a micrometer. A bed was prepared by packing a weighed quantity of the glass into the permeability measuring tube with constant stirring, to obtain as nearly as possible random orientation. The results of a permeability determination with water were as follows:

Average diameter of rods = 0.0407 cm.

Ratio of length to diameter of rods  $\frac{1}{d}$  = 20

Diameter of permeability measuring tube = 1.91 cm.

Depth of bed of glass rods = \$.00 cm.

Porosity of bed = 0.685

Average value of  $K\nu = 4.78 \times 10^{-2}$ 

Specific surface (uncorrected) = 115 sq. cm./cc.

Wall correction = 3.0 sg. cm./cc.

Specific surface (corrected) = 112 sq. cm./cc.

True specific surface  $\frac{\pi dl + \pi \frac{d^2}{2}}{\pi \frac{d^2}{1}} = \frac{101 \text{ sq. cm./cc}}{100 \text{ sq. cm./cc}}$ 

Ratio of calculated specific surface to true specific surface =  $\frac{1.11}{1}$ 

## (d) Measurements with Copper Wire

A somewhat greater ratio of length to diameter for the constituent particles was obtained by the use of 5 millimeter lengths of No. 38 enamelled copper wire. A bed of this material was formed with constant stirring to obtain random orientation of the wires. The permeability of the bed to water was then measured in the usual manner.

Diameter of wire = 0.01017 cm.

Ratio of length to diameter  $\frac{1}{d} = 50$ 

Diameter of permeability measuring tube = 1.91 cm.

Depth of bed of wire = 12.00 cm.

Porosity of bed = 0.830

Average value of  $K\nu = 2.14 \times 10^{-2}$ 

Specific surface (uncorrected) = 433 sq. cm./cc.

Wall correction =  $\frac{2}{.170 \times 191}$  = 6.2 sq. cm./cc.

Specific surface (corrected) =  $\frac{427 \text{ sq. cm./cc.}}{}$ 

True specific surface (neglecting area of ends) =  $\frac{4}{d}$ 

= 394 sq. cm./cc.

Ratio of calculated specific surface to true specific surface =  $\frac{1.08}{1.08}$ 

# (e) Measurements with Glass Wool

To secure higher porosities and still greater ratios of length to diameter for the constituent particles, beds were prepared from ordinary glass wool. For this purpose the most compact and uniform bundles of glass fibers were

selected from a large quantity of glass wool. The bundles were stretched and rolled to bring the fibers to a parallel position, and were then cut into the required lengths with shears. Two different ratios of length to diameter were obtained by cutting the fibers into lengths of 1 1/2 and 6 millimeters.

The true specific surface of the material was estimated from the perimeters and cross-sectional areas of a random sample of fibers. Paraffin-black sections of the fibers were prepared for examination with a micrometer microscope. The fiber outlines were subsequently plotted on graph paper for measurement of areas and perimeters.

Since it was expected that particles of this type would show a decided tendency toward orientation during the packing process, beds of glass fibers were prepared in two different ways. In the first series, beds were prepared by feeding the fibers into the dry permeability measuring tube, stirring constantly to obtain random packing. Water or benzene was then added and entrained air was removed by reducing the pressure above the liquid. In the second series, the permeability tube was filled with water before the addition of the glass fibers. The fibers were suspended in the water by vigorous stirring and were then allowed to It was assumed that preferential orientation in horisettle. zontal planes would be produced in the latter case, and that a comparison of the two results would indicate whether the effect

were significant.

The results of the permeability determinations are summarized in Table V. The wall correction has been omitted throughout in view of its negligible size for large specific surfaces. The values listed for the product  $K\nu$  are in each case the average for 10 or more permeability measurements. As with sand grains, a general trend toward decreased  $K\nu$  with increased flow rate was noted in each series. The trend was of the order of the experimental error (i.e. a decrease of 3% in  $K\nu$  for a range in flow rates of 3 to 1), but was clearly evident.

Table V shows that slightly higher values of calculated specific surface are obtained when the constituent fibers are allowed to orient themselves by settling from suspension. The results also show that the calculated specific surface obtained by the use of benzene is approximately 6% lower than that obtained by the use of water; this effect is similar to that noted with sand grains.

# (f) Measurements with Corning Fiberglass

A close approach to natural fiber dimensions, together with a very large departure from spherical form, was
obtained by the use of Corning Fiberglass No. 008. This
material was received from the manufacturer in the form of
a thin mat of long fibers, from which bundles of nearly
parallel fibers could be produced by rolling and stretching.
These bundles were cut into 1 1/2 or 8-10 millimeter lengths,

TABLE V

Permeability Measurements with Glass Wool

Fiber Length (mm.)	Ratio $\frac{1}{d}$	Method of Packing	Liquid	Average $K \nu$	Porosity	Calculated Specific Surface (sq. cm./cc.)
6	200	random	benzene	4.70x10 <sup>-3</sup>	0.910	1965
6	200	random	water	2.95x10 <sup>-3</sup>	0.895	2090
6	200	settling	water	1.106x10 <sup>-3</sup>	0.846	2130
1 1/2	50	settling	water	1.294x10 <sup>-3</sup>	0.857	2165

True specific surface from microscopic examination =  $2000^{\pm}$  100 sq. cm./cc.

TABLE VI
Permeability Measurements with Corning Fiberglass

Fiber Length	Ratio <u>1</u>	Liquid	Average $\mathbf{K}\nu$	Porosity	Calculated Specific Surface (sq. cm./cc.)
1 1/2 mm.	200	benzene	2.32x10-4	0.885	6660
8 - 10 mm.	1000	benzene	4.08x10-4	0.919	7540
>100 cm.	> 105	benzene	5.30x10 <sup>-4</sup>	0.928	7560
>100 cm.	>105	water	4.97x10-4	0.930	8070

True specific surface from microscopic examination =  $7000 \pm 400$  sq. cm./cc.

yielding fibers with ratios of length to diameter of 200 of 1000 respectively. An extreme case was also investigated in which the unravelled strands were used in their original length of 100 to 200 centimeters.

Beds were formed by packing the fiberglass into a dry permeability tube, adding water or benzene, and repeatedly reducing the pressure above the surface of the liquid to remove entrained air. The cross-sectional areas and perimeters of a number of glass fibers were measured microscopically to enable calculation of the true specific surface.

The results of permeability measurements with benzene and water are presented in Table VI. Their results show an increase in calculated specific surface with increased ratio of length to diameter. As in previous cases the specific surface derived from permeability measurements with benzene is approximately 6% lower than that obtained with water.

# (g) Measurements with a Mixture of Glass Fibers

A wide variation of fiber diameters is present in many naturally occurring fibrous materials. It was thus considered desirable to obtain information on the validity of the Kozeny equation where such a size range existed. A mixture of approximately equal weights of fiberglass and ordinary glass wool, each in 1 1/2 millimeter lengths, was prepared. The permeability to water of a bed of this material was determined in the usual manner.

Diameter of largest fiber = 0.035 mm.

Diameter of smallest fiber = 0.0052 mm.

Average  $K\nu = 7.62 \times 10^{-4}$ 

Porosity  $\varepsilon = 0.909$ 

Calculated specific surface  $S_0 = 4830$  sq. cm./cc. True specific surface =  $4700 \pm 300$  sq. cm./cc.

## (h) Measurements with Celanese Yarn

Celanese yarn, a material of diameter comparable to glass wool but with an entirely different type of surface was selected for the final investigation. The yarn was cut into 5 millimeter lengths and was then unravelled by rubbing. The permeability to benzene of a bed formed from the fiber mass was determined in the usual way.

The true specific surface was estimated from microscopic examination of a number of fiber cross sections. The areas and perimeters of these sections were measured from drawings on squared paper. The forms most frequently encountered were irregular, corrugated cylinders. Due to the complexity of the cross sections, the accuracy of the measurements was not better than \$\pm 20\%.

A complication introduced by the use of celanese was the possible change in fiber dimensions with moisture content. For this reason benzene was employed for the permeability determinations and for measurement of the superficial density of the fibers by the displacement method. While no confirmatory measurements were made, it was assumed

that no significant change in fiber dimensions or moisture content would occur during the short period of the experiment.

The results obtained from permeability measurements with two separate beds of celanese fibers are summarized in Table VII.

## (i) Discussion of Results

Substantial agreement is shown between the values of specific surface calculated from permeability determinations and from the geometry of the constituent particles in all of the preceding investigations. With materials most nearly simulating natural fibers, such as celanese and fiberglass, the agreement is actually within the accuracy of the geometrical measurement. It is therefore indicated that equation (18), the Kozeny-Carman equation is valid for an extensive range of particle shapes and sizes.

Several additional points are worthy of note.

The presence of more than one size of particle (at least for two sizes in approximately equal quantities) does not affect the applicability of the equation. Indeed, in a recent paper Carman (36) has shown that satisfactory agreement is obtained with mixtures of very wide size range.

Using three samples of spherical glass particles of diameters 2 to 40 microns, 10 to 90 microns and 10 to 140 microns, agreement with ±2% was found between the calculated

## TABLE VII

# Benzene Permeability Measurements with Celanese Yarn

Fiber Length	Ratio $\frac{1}{d}$	Average Kv	Porosity	Calculated Specific Surface(sq.cm./cc)
5 mm.	200	1.574x10-3	0.898	2950
5 mm.	200	1.749x10-3	0.904	<b>29</b> 90

True specific surface from microscopic examination = 3000 ± 600 sq. cm./cc.

and true values of specific surface. It is thus not improbable that satisfactory results may be obtained with fibrous materials of considerable size range.

Non-uniform packing of the bed does not appear to be a troublesome factor, even though discontinuities must occur with the more elongated particles. This is striking in view of the wide variation of the porosity function  $\frac{\epsilon^3}{(1-\epsilon)^2}$  of the Kozeny equation with relatively small changes in the porosity  $\epsilon$ . It had been feared that the effect of the more closely packed portions of the bed on the permeability would not be counterbalanced by the looser sections.

The effects of particle orientation may be noted in certain of the results of the preceding investigations. The value of the proportionality constant k of equation (17) was chosen as 0.20 by Carman from analysis of data on nearspherical particles such as sand grains. In such cases all orientations are nearly equally probable. However, for a bed of rod-like particles the permeability will obviously be much less if all are packed with their long axes normal to the direction of flow than if packed parallel to the direction of flow. Fowler and Hertel (28) have deduced that k should be approximately equal to  $(\frac{\sin^2 \phi) \text{Av}}{3}$ , where of taken as the angle between the direction of macroscopic flow and the normal to an element of surface exposed to the On this basis, k would depend directly on the

orientation of the particles comprising the bed, and would have the following values:

For a bed of spheres 
$$k = \frac{2/3}{3} = 0.22$$
  
For cylinders parallel to flow  $k = \frac{1}{3} = 0.33$   
For cylinders normal to flow  $k = \frac{1/2}{3} = 0.17$ 

The constant K in the Kozeny-Carman equation (18) would therefore have the values 14.7, 18.1 and 12.8 respectively.

With rod-like particles, ordinary methods of bed formation should favor orientation in the horizontal direction, resulting in decreased permeability and increased apparent specific surface. The results of the preceding investigations with elongated particles do show a calculated specific surface slightly greater than the true specific surface whenever the true surface area was measured with sufficient accuracy for the effect to be detectable. The difference is particularly noticeable with glass wool, where orientation was purposely introduced by allowing the fibers to settle in water.

The effects of particle orientation might be expected to be very significant with natural fibers where the horizontal orientation would be increased by compression of the bed. This factor would require careful investigation before the Kozeny-Carman equation could be applied to mea-

surements with wood-pulp or similar fibers.

The chemical composition of the solid particles appears to exert no significant influence on the permeabilityspecific surface relationship. However, a slight difference is found between the values of specific surface calculated from permeability measurements with polar and non-polar liquids, e.g. water and benzene. On theoretical grounds, the nature of the solid and liquid would not be involved unless a stationary layer of liquid of significant thickness were in contact with the solid surfaces. In that event. different thicknesses of the stationary layer might be expected with different combinations of solid and liquid. effect would obviously be greater with small particles where the reduction of the effective pore diameter would be relatively large. This problem is discussed more fully in Part Ib, where comparisons are made of the permeability values obtained with a variety of liquids and gases.

A trend toward decreasing values of the product  $K\nu$  with increasing flow rate, in a series of runs on one bed of material, is apparent in many cases. Investigation of this effect is difficult since the overall decrease in  $K\nu$  is of the same order as the experimental error. Carman (3) has shown that the permeability-specific surface relationship fails for values of the ratio  $\frac{Q}{A\nu S_0(1-\epsilon)}$  greater than  $\frac{A\nu S_0(1-\epsilon)}{20}$  or less than  $10^{-3}$ . However, in the series of runs with 20 to 28 mesh sand the decrease is clearly shown, but the ex-

 $\frac{Q}{AUS_0(1-\epsilon)}$  are only 0.41 and 0.85. The treme values of possibility of a reduction in the thickness of the stationary layer of liquid in contact with the solid surface with an increase in liquid velocity has been discussed by Carman (3), Darapsky (23) and others. However, in this event an increase in the flow rate would result in an increase in the value of The only remaining explanation is the head loss due to turbulence and velocity changes in the permeability measuring tube. With streamline flow, friction forces external to the bed appear as a fixed increase in the resistance of the bed, since both are functions of the first power of the velocity. However, inertial forces are expressed as higher powers of the velocity, resulting in a continuous decrease of  $K\nu$  with increasing velocity.

# (j) Refinements of Technique for Routine Measurement of Liquid Permeability

The apparatus shown in Figure 1 was designed for research purposes where flexibility and ease of observation were basic requirements. Various modifications may be made to advantage in constructing an instrument for routine use with any one type of material. A suggested design for such an instrument is shown in Figure 2.

The bed of solid material is contained in a brass tube A. This tube is fitted with a liquid inlet connection B and is threaded into a brass base C. The bed is supported on a circle of copper gauze D and a metal grid E. The grid is constructed of thin strips of brass silver-soldered into

an outer ring, as shown in the auxiliary view of Figure

2. The grid rests on a shoulder F when the tube is
threaded into the base.

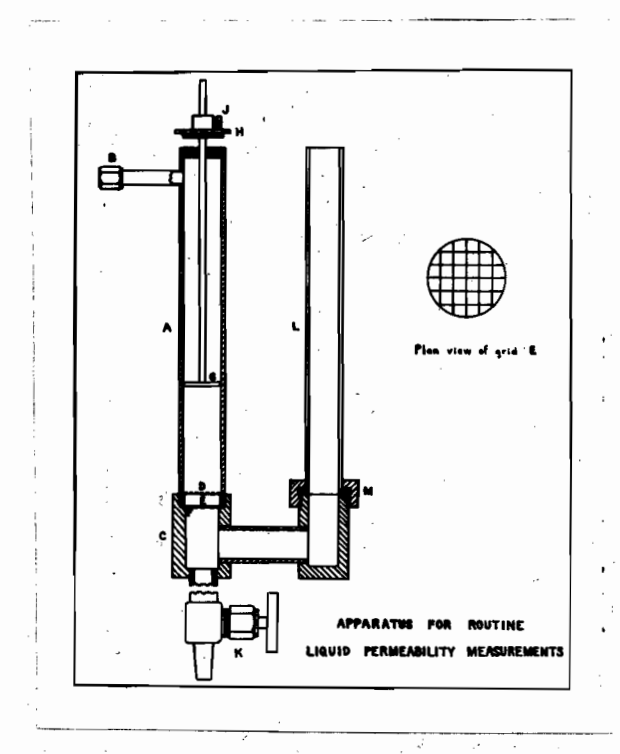


Figure 2

The depth of the bed is measured by means of the plunger G. This plunger bears a perforated disc at the lower end to rest on the top of the bed. The stem of the plunger passes through a cap H, which is threaded into the top of the tube. The depth of the bed is read directly on a scale on the stem of the plunger. The plunger is also useful for maintaining a definite depth of bed with loose or springy materials. In such cases the plunger is

clamped by the set screw J and is left in place during the permeability measurement. The resistance of the perforated disc will normally be negligible with the type of material requiring compression.

The rate of flow through the bed is controlled by the 1/8 inch needle value K. The head of liquid at the lower side of the bed is measured on the glass side tube L. Since the head of liquid in tube A is constant, tube L may be calibrated directly in terms of head loss across the bed. Tube L is connected to the base C by means of a lock nut and gasket M.

The liquid supply system may be similar to that shown in Figure 1, but need not be adjustable in height.

The two units should be connected by means of a flare or compression type coupling to facilitate removal for cleaning.

An instrument constructed as above possesses the advantages of ruggedness, accuracy of dimensions and ease of cleaning. Any non-corrosive liquid may be employed by a suitable choice of gaskets and value packing. The dimensions of the apparatus may be varied between wide limits to suit the material under investigation.

# (k) Construction of Nomographs for Liquid Permeability Calculations

The calculation of specific surfaces from liquid permeability data by means of the Kozeny-Carman equation is relatively laborious. However, in a series of measurements with one bed of material the only variables involved are the

rate of flow, the head loss, and the kinematic viscosity of the liquid. A nomograph may thus be constructed for calculation of the specific surface from these variables and from the constant factor involving the dimensions of the bed and the volume of solid material. By this means much time may be saved where a series of runs are carried out with one bed of material.

Nomographs may also be constructed for calculation of the constant factor mentioned above. Unfortunately, the rapid change of the porosity function  $\frac{\epsilon^3}{(1-\epsilon)^2}$  with a small change in porosity makes it difficult to obtain accuracy with a chart of reasonable dimensions.

The construction of the nomographs may be carried out in the following manner:

Let the volume of solid material in the bed # V cc.

" diameter of the bed = D cm.

" " depth " " " = L cm.

Total volume of bed =  $\frac{\pi D^2 L}{\mu}$  cc.

Pere volume in bed =  $\frac{nD^2L}{4} - V$  cc.

Porosity 
$$\varepsilon = \frac{\frac{\pi D^2 L}{4} - V}{\frac{\pi D^2 L}{h}} = 1 - \frac{4V}{\pi D^2 L}$$

Permeability  $K = \frac{QL}{Ah} = \frac{4QL}{\pi D^2 h}$  (from equation (16).)

The Kozeny-Carman equation 
$$S_0 = 14 \sqrt{\frac{1}{K\nu} \cdot \frac{\epsilon^3}{(1-\epsilon)^2}}$$
 may then be written  $S_0 = 14 \sqrt{\frac{\pi D^2 h}{4QLV} \cdot \frac{(1-\frac{4V}{\pi D^2 L})^3}{(\frac{4V}{\pi D^2 L})^2}}$  (21)

Stage I Calculation of the powesity function

$$\frac{\left(\frac{dD_3\Gamma}{d\Lambda}\right)_3}{\left(1-\frac{dD_3\Gamma}{d\Lambda}\right)_3} = \nabla:$$

Let 
$$\frac{\mu V}{\pi D^2 L} = \Phi$$
  
 $\log \Phi = \log \frac{\mu}{\pi} + \log V - 2 \log D - \log L$   
Let  $2 \log D + \log L = \theta$  (1)  
Then  $\theta + \log \Phi = \log V + \log \frac{\pi}{4}$  (2)

(1) 
$$x = m_1 (2 \log D)$$
  
 $y = m_2 (\log L)$   
 $z = m_3 \theta$ 

Let D vary from 1 to 10 cm.

If  $\underline{m_1} = 5$ ,  $x = 10 \log D$ , and D scale is 10 units long. Let L vary from 0.5 to 50 cm.

If  $m_2 = 5$ ,  $y = 5 \log L$ , and L scale is 10 units long.

Then 
$$m_3 = \frac{m_1 m_2}{m_1 + m_2} = 2.5$$

$$x = 10 \log D$$

$$y = 5 \log L$$

$$z = 2.5 \theta$$

$$z = m_3 \theta$$

 $a = m_4 \log \phi$ 

 $b = m_5 \log V$  (omitting  $\frac{\pi}{4}$  until scales are located)

Let  $\phi$  vary from 0.01 to 1.0

If  $\underline{m_4} = 5$ ,  $\underline{a} = 5 \log \phi$ , and  $\phi$  scale is 10 units long Then  $\underline{m_5} = \frac{\underline{m_3 m_4}}{\underline{m_3} + \underline{m_4}} = 1.667$ 

$$\therefore z = 2.5 \theta$$

 $a = 5 \log \phi$ 

 $b = 1.667 \log V$ 

The chart is constructed as shown in Figure 3. It will be noted that the positions of the  $\phi$  and V scales have been interchanged to obtain a more open  $\phi$  scale. A starting point for the V scale is located by setting D = 2.0, L = 31.8 and  $\phi$  = 0.1, when V = 10.0.

Since the porosity function  $\frac{(1-\phi)^3}{\phi^2}$  is required for the succeeding calculations, the values of this function are plotted directly on one side of the  $\phi$  scale. This is most easily done by constructing a curve of  $\frac{(1-\phi)^3}{\phi^2}$  against  $\phi$  on log paper, and then selecting the values of  $\phi$  corresponding to integral values of  $\frac{(1-\phi)^3}{\phi^2}$ . The symbol  $\Delta$  will be used in the remainder of this section to denote the porosity function  $\frac{(1-\phi)^3}{\phi^2} = \frac{\epsilon^3}{(1-\epsilon)^2}$ .

## Stage II

Calculation of the constant factor for a given bed of material:

$$S_0 = 14\sqrt{\frac{\pi D^2 h \Delta}{4QL \nu}}$$
 from equation (21)

Let 
$$n = 14\sqrt{\frac{D^2\pi\Delta}{4L}}$$

Then 
$$S_0 = n\sqrt{\frac{h}{Q\nu}}$$
 (22)

And n incorporates all the factors which are constant for a given bed of solid material.

$$n = 14\sqrt{\frac{\pi \overline{D^2\Delta}}{4L}} = 12.4 \quad D\sqrt{\frac{\Delta}{L}}$$

 $\log n = \log 12.4 + \log D + 1/2 \log \Delta - 1/2 \log L$ 

Let 
$$\log D - 1/2 \log L = \theta$$
 (1)

Then  $\theta + 1/2 \log \Delta = \log n - \log 12.4$  (2)

(1) 
$$x = m_1 \log D$$

$$y = -m_2 (1/2 \log L)$$

$$z = m_3 \theta$$

Let D vary from 1 to 10 cm.

If  $\underline{m_1} = 10$ ,  $x = 10 \log D$ , and D scale is 10 units long Let L vary from 0.5 to 50 cm.

If  $m_2 = 10$ ,  $y = -5 \log L$ , and L scale is 10 units long

Then 
$$m_3 = \frac{m_1 m_2}{m_1 + m_2} = 5$$

$$x = 10 \log D$$

$$y = -5 \log L$$

$$z = 5 \theta$$

(2) 
$$z = ms \theta$$

$$a = m_4 (1/2 \log \Delta)$$

$$b = ms \log n \text{ (omitting 12.4 until scales are located)}$$

Let  $\Delta$  vary from 0.2 to 2000

If  $\underline{m_4} = 5$ ,  $a = 2.5 \log \Delta$ , and  $\Delta$  scale is 10 units long

Then 
$$m_5 = \frac{m_3 m_4}{m_3 + m_4} = 2.5$$

$$\therefore z = 5 \theta$$

$$a = 2.5 \log \Delta$$

$$b = 2.5 \log n$$

The chart is constructed as shown in Figure 4. A starting point for the n scale is located by setting D=2.01, L=5.0 and  $\Delta=20$ , when n=50.

## Stage III

Calculation of the specific surface:

$$S_0 = n \sqrt{\frac{h}{Q \nu}}$$
 (equation 22)

 $\log S_0 = \log n + 1/2 \log h - 1/2 \log Q - 1/2 \log v$ 

Let 
$$1/2 \log h - 1/2 \log Q = p$$
 (1)

And let 
$$p - 1/2 \log \nu = q$$
 (2)

Then 
$$q + \log n = \log S_0$$
 (3)

(1) 
$$x = m_1 (1/2 \log h)$$
  
 $y = -m_2 (1/2 \log Q)$   
 $z = m_3 p$ 

Let h vary from 0.1 to 20 cm.

If  $\underline{m_1} = 10$ ,  $x = 5 \log h$ , and h scale is 11.5 units long Let Q vary from 0.01 to 10 cc./sec.

If  $m_2 = 10$ ,  $y = -5 \log Q$ , and Q scale is 15 units long

Then 
$$m_3 = \frac{m_1 m_2}{m_1 + m_2} = 5$$

$$x = 5 \log h$$

$$y = -5 \log Q$$

$$z = 5 p$$

(2) 
$$z = ms p$$

$$a = -m_4 (1/2 \log v)$$

$$b = ms q$$

Let  $\nu$  vary from 0.001 to 0.1 sq. cm./sec.

If  $\underline{m_4} = \underline{10}$ ,  $a = -5 \log \nu$ , and  $\nu$  scale is 10 units long

Then 
$$m_5 = \frac{m_3 m_4}{m_3 + m_4} = 3.33$$

$$z = 5 p$$

$$a = -5 \log \nu$$

$$b = 3.33 q$$

(3) 
$$b = m_5 q$$

$$c = m_6 \log n$$

$$d = m_7 \log S_0$$

Let n vary from 10 to 104

If  $m_6 = 5$ ,  $c = 5 \log n$ , and n scale is 15 units long

Then 
$$m_7 = \frac{m_5m_6}{m_5 + m_6} = 2.0$$

b = 3.33q

 $c = 5 \log n$ 

 $d = 2 \log S_0$ 

The chart is constructed as shown in Figure 5. A starting point for the  $S_0$  scale is located by setting h=1.0, Q=1.0,  $\nu=10^{-2}$  and  $n=10^{-3}$ , when  $S_0=10^4$ .

The charts of Figures 3, 4 and 5 should be constructed with a unit length of at least 1, and preferably 2 inches. The resulting maximum heights of the charts are then 15 and 30 inches respectively. The accuracy normally possible with a 2 inch unit length is  $\pm 3\%$  for  $\Delta$ ,  $\pm 1\%$  for n and  $\pm 2\%$  for So. The resulting  $\pm 6\%$  cumulative error in calculating So entirely by the use of the charts is somewhat greater than the experimental error. It is therefore generally advisable to calculate the constant factor n by logarithms and use the chart of

Figure 5 for the final stage only. However, for approximate work with a variety of materials much time may be saved by the use of the charts for the complete calculation.

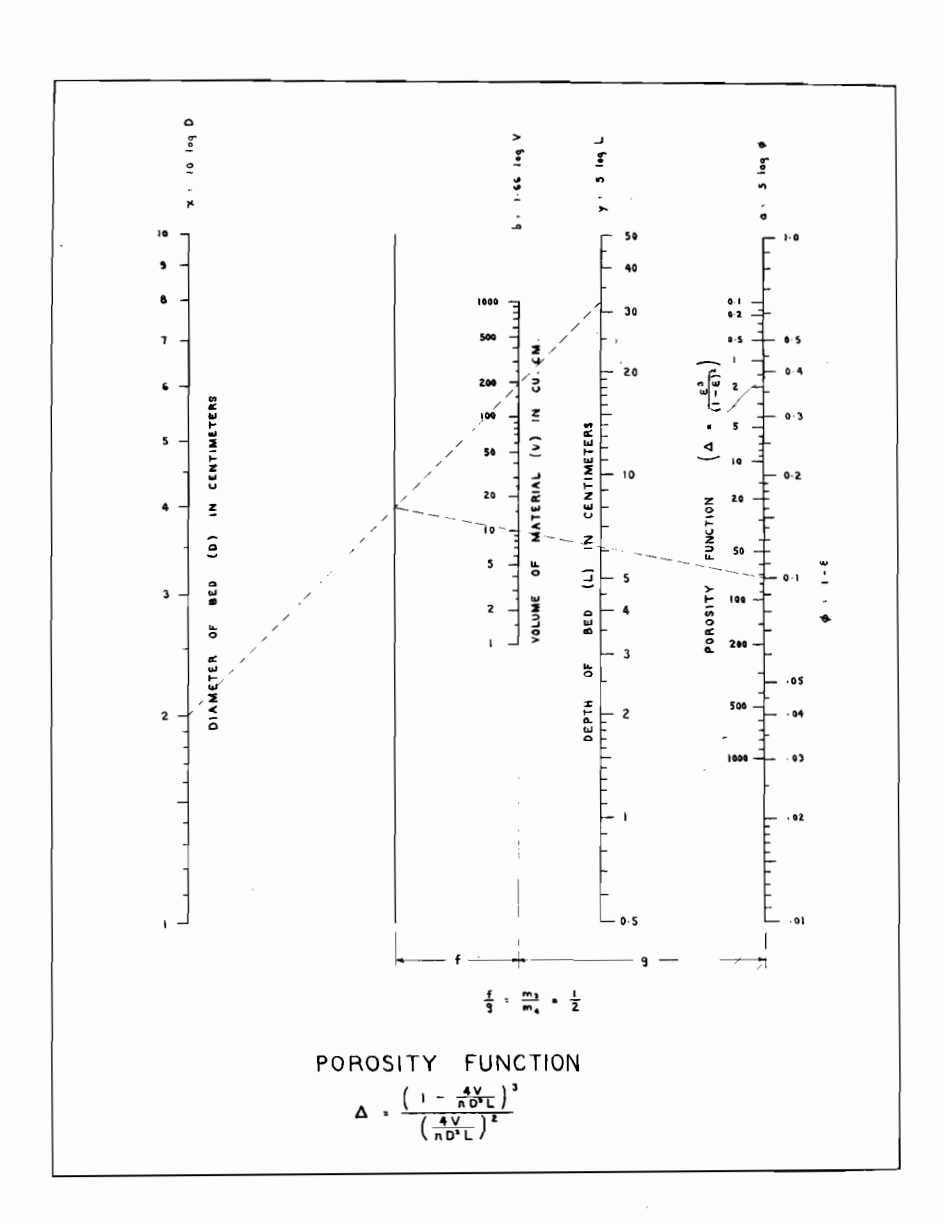


Figure 3.

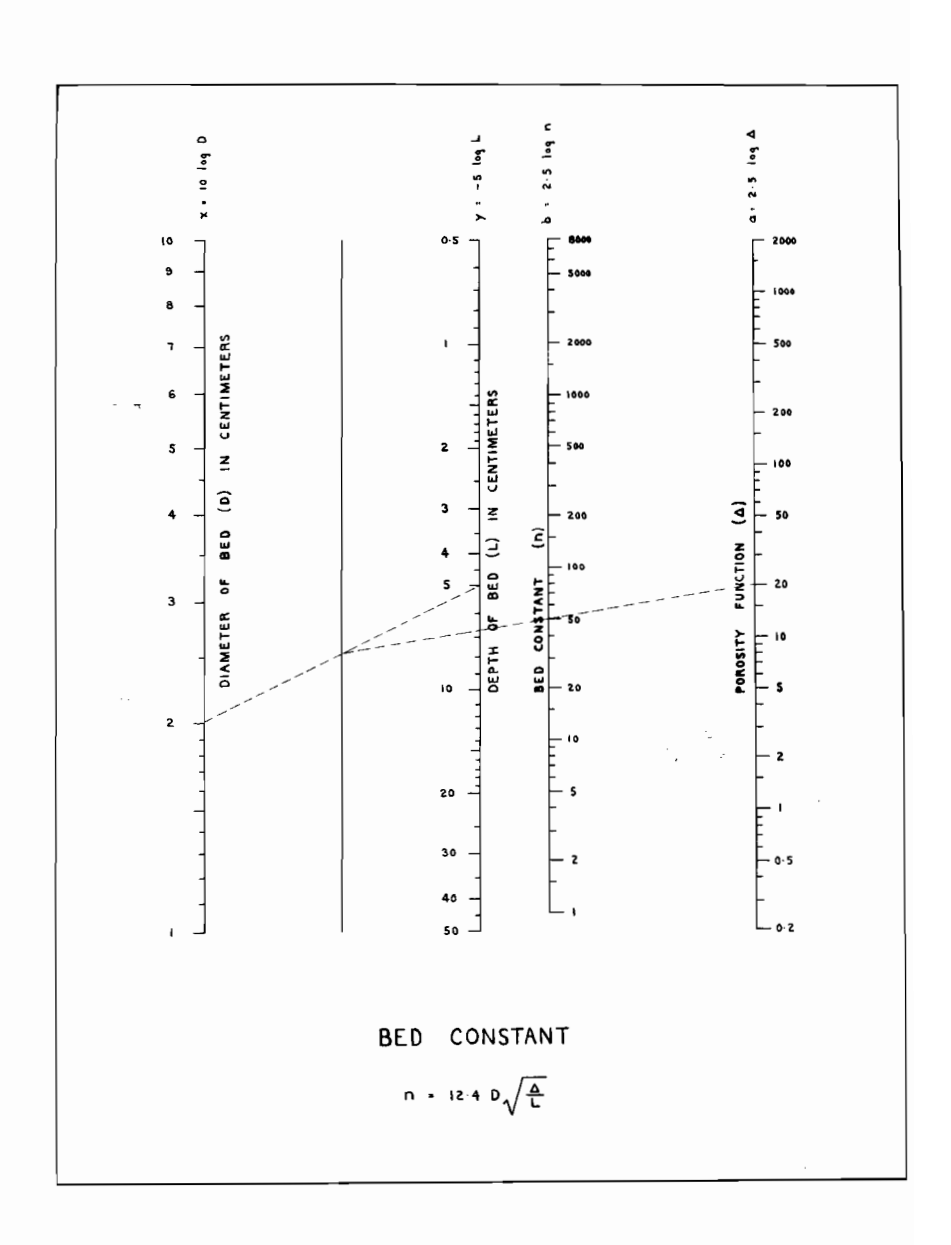


Figure 4.

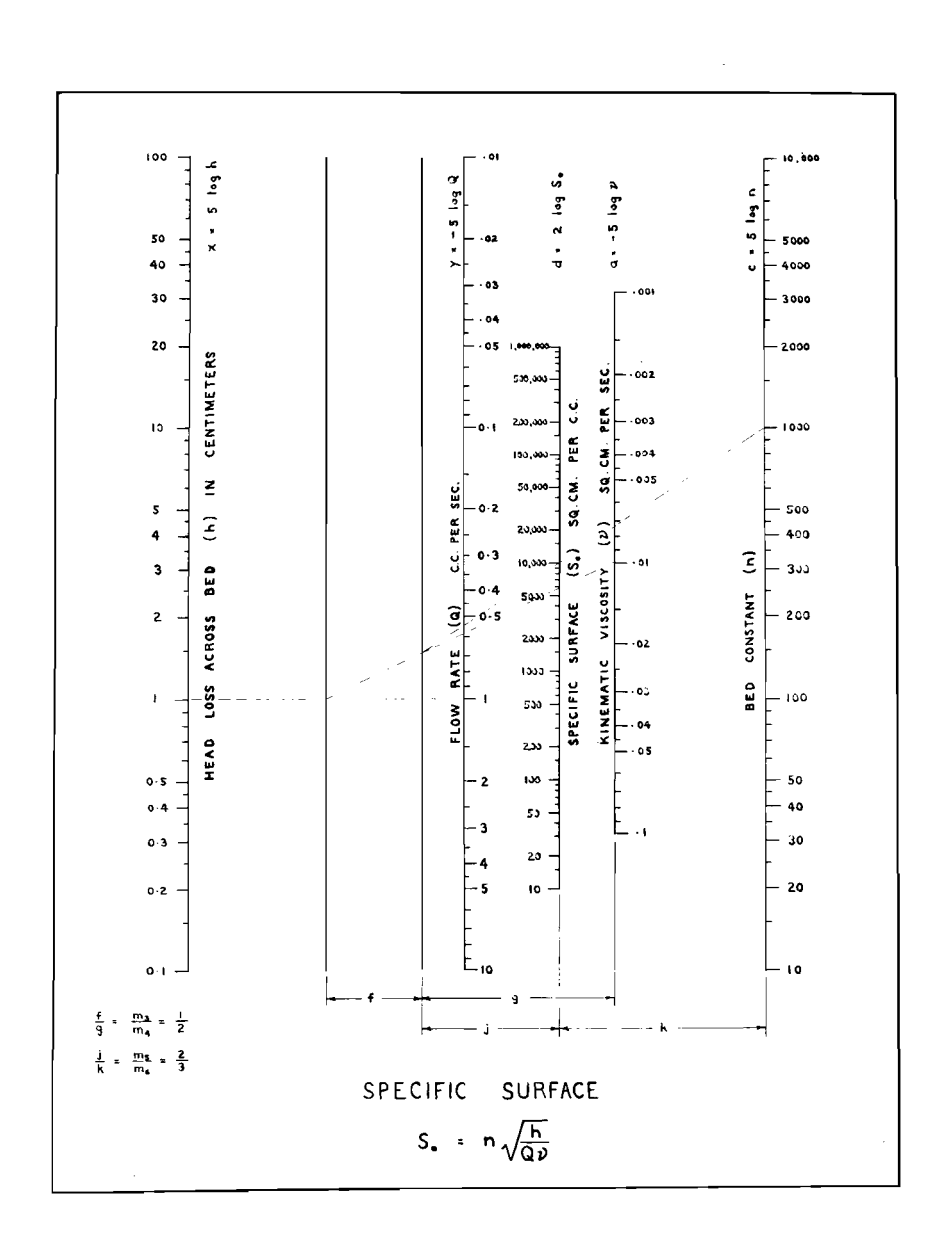


Figure 5.

# PART Ib

Measurement of Specific Surfaces by the Gas Permeability Method

#### 1. INTRODUCTION

The theoretical development of the Kozeny equation suggests no restrictions as to the nature of the fluid. However, as briefly mentioned in Part Ia, it is probable that the true picture of flow through a porous medium is not cuite identical with that consider-The notion of a "boundary layer" ed in the derivation. is common to all flow problems, whether a material fluid or heat energy be under consideration. For the case of fluid flow, it has been postulated that all solid surfaces are enveloped by an immobile layer of fluid, the actual flow taking place outside this boundary layer. The effective diameter of a stream channel in a porous medium is then the true diameter reduced by the depths of the stationary layers on the particles bounding the channel. bility of the bed, and thus the calculated specific surface, is dependent on the effective dimensions of the stream chan-Since the thickness of the boundary layer will pronels. bably vary with the nature of the fluid, it is logical to expect that the values of calculated specific surface obtained with various liquids and gases will not be identical.

The actual dimensions of the boundary layers have been the subject of some controversy. The existence of stagnant regions may be logically ascribed to forces of adsorption between the fluid and the solid. On this basis,

Carman has assumed layers of molecular dimensions, i.e.,  $10^{-8}$  centimeters. Other investigators, however, have provided evidence that the thickness of stagnant liquid layers is much greater than this value. For cements with specific surfaces of the order of 4000 sq. cm./cc., Lea and Nurse (37) found that the specific surfaces calculated from liquid permeability data were uniformly higher than those calculated from gas permeability data by a factor of 1.3 to 1.4. The liquid employed in these investigations was a 2% solution of calcium chloride in ethanol, the gases were hydrogen, nitrogen, carbon dioxide and air. For such a cement the mean particle diameter would be greater than  $10^{-3}$  centimeters, so that a  $10^{-8}$  centimeter layer could exert no significant effect.

One criticism has been made of the above results: with a material containing a wide range of particle sizes, such as cement, size separation may contribute to the low permeability found with liquids. During formation of the bed by stirring the cement powder into the liquid, fine particles will be concentrated in the top layer thus reducing the overall permeability and increasing the apparent specific surface. However, large differences have also been reported by Bozza and Secchi (38) between the permeabilities of fine quartz sand and powdered galena to various liquids. The permeabilities to aqueous solutions were

found to be approximately 30% greater than those to organic liquids. Significantly greater permeabilities to air than to water have been noted by Green and Ampt (39) with beds of glass spheres, where sedimentation was almost certainly absent.

The presence of stationary fluid layers obviously limits the field of application of the permeability method of surface area measurement. However, the thinner these layers, the smaller are the channels and the larger are the specific surfaces for which the method may be used. It is reasonable to expect that the boundary layers would be much thinner with gases than with liquids, so that a gas permeability method would be applicable to larger specific Lea and Nurse (37) concluded from their investigations that liquid permeability measurements were suitable only for specific surfaces up to 1000 sq. cm./cc., while air permeability measurements were satisfactory to at least 4000 sa. cm./cc. With cements having specific surfaces of 3000 to 4000 sq. cm./cc., reproducible results were obtained with four different gases over a wide range of flow rates. Further, the values of specific surface calculated from gas permeabilities by means of the Kozeny equation were within \$\pm2\% of those computed by the Heywood method, using the Andreasen cubical definition of particle diameter.

It should also be noted that the gas permeability method possesses great advantages in the matter of bed

formation. The preparation of an air-free bed for liquid permeability determinations is a serious problem with all fine powders and fibrous materials. In the case of natural fibers, selection of a liquid which will not disturb the original fiber structure and orientation is also difficult. No such problems are encountered in the preparation of a sample for gas permeability measurements.

The investigations to be described in the next section are largely devoted to a comparison of the values of specific surface obtained by measurements of the permeabilities of a variety of materials to liquids and to gases. The surface areas are in the range in which Lea and Nurse observed considerable divergence between gas and liquid permeability results. It was hoped in this way to establish the limits of usefulness of the liquid and gas permeability methods for measurement of large specific surfaces, especially of fibrous materials.

Unfortunately, this objective was not completely attained in the investigations to be described. The outbreak of hostilities made it desirable to undertake the measurement of the specific surfaces of materials of military significance. This immediate requirement made it impossible to complete a thorough investigation of the gas permeability method.

## 2. EXPERIMENTAL PROCEDURE AND RESULTS

#### (a) Apparatus and General Procedure

The apparatus employed for the measurement of gas permeability is shown in Figure 6. This assembly differs from the liquid permeability apparatus in the use of a capillary flowmeter to measure the rate of gas flow, and in the use of a manometer to measure the pressure drop across the bed. Accessory equipment is also required to maintain a flow of dry gas at constant temperature and pressure.

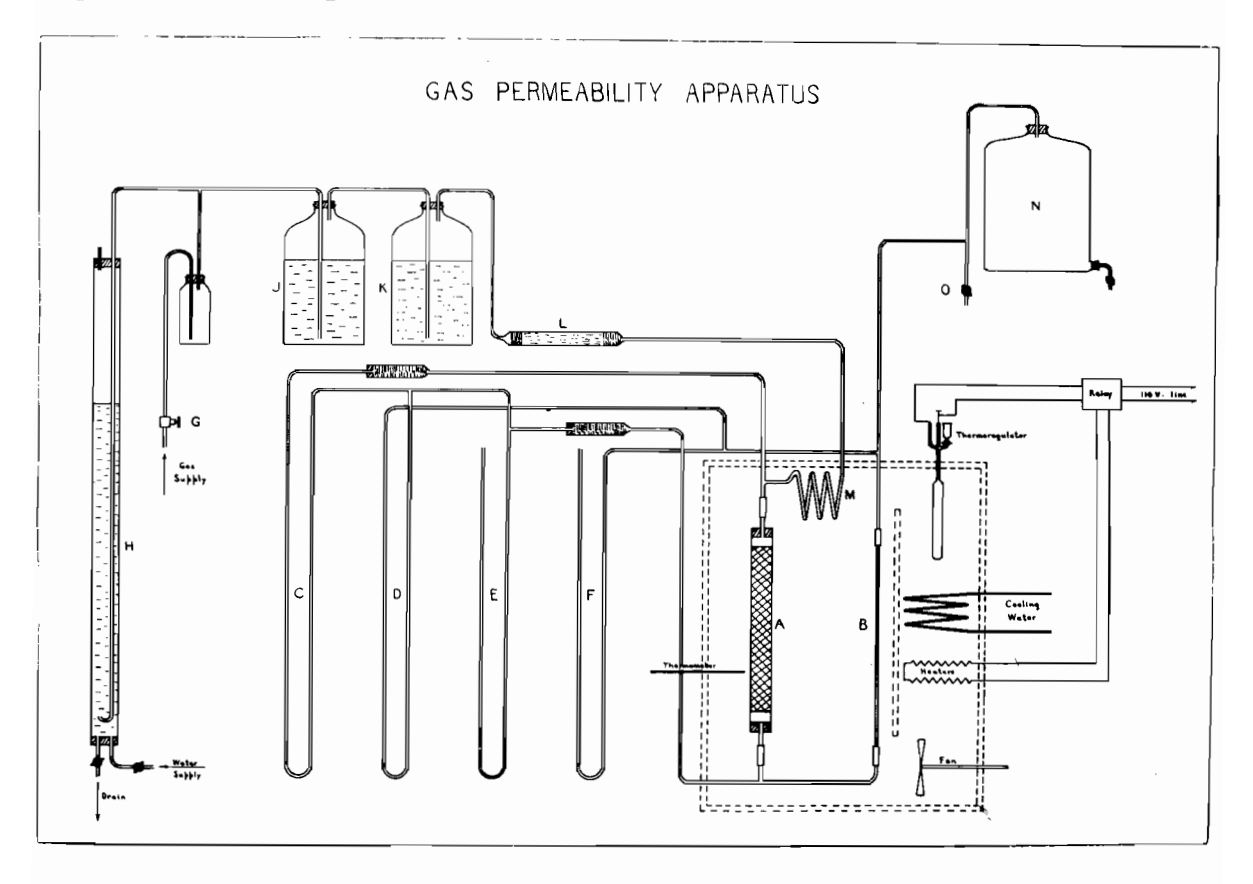


Figure 6.

Referring to Figure 6, the permeability tube A comprises a length of uniform glass tubing closed with rubber stoppers at both ends. A spiral of sheet brass and a disc of copper gauze support the bed of solid material as in the liquid permeability apparatus. A capillary flowmeter B is connected in series with the permeability measuring tube. Water manometers C and D are arranged to indicate the pressure drops across the bed of material and across the flowmeter, respectively. the use of four sizes of capillary flowmeters a wide range of flow rates can be measured with accuracy. Open tube manometers E and F are also provided to indicate the pressures at the inlet and outlet of the capillary flowmeter. While not essential for routine work, these are helpful in showing the actual pressures in the system during preliminary runs and flowmeter calibration.

The gas flow is controlled by the needle value G, connected to a source at 10 to 25 pounds per square inch pressure. The water column H provides pressure regulation at the discharge side of the needle value. The level of water in this column is adjusted to obtain the necessary pressure for each flow rate. With steady sources of compressed gas it is often possible to dispense with the water column, thus reducing the time required for a series of permeability measurements.

The gas stream is dried by passage through two

bottles J and K containing concentrated sulphuric acid, and through a phosphorus pentoxide tube L. A plug of fiberglass is inserted in the outlet end of the phosphorus pentoxide tube to remove dust. The gas finally passes through a coil of copper tubing M for temperature adjustment before entering the permeability tube.

The permeability tube A, the capillary flowmeter B, and the copper coil M are enclosed in a constant temperature air bath. The bath is fitted with cooling coils and electric heating elements so that temperatures above or below that of the room may be maintained. A fan and a vertical baffle provide rapid circulation of air to all parts of the bath. The bath is constructed of one-inch lumber and is covered with three layers of asbestos paper for additional insulation. Temperature control within ±0.2°C. is obtained throughout the bath by this means.

A 20 liter water reservoir N is provided for calibration of the capillary flowmeters. Gas may be drawn through the flowmeter at a known rate by closing stopcock O and draining water from N. The gas supply pressure is adjusted by means of the water column H so that the pressure indicated by manometer F is equal to that of the atmosphere. Calibration curves for each flowmeter are constructed for each gas to be used in the permeability measurements.

# (b) Calculation of Specific Surface from Gas Permeability Data

The Kozeny-Carman relation must be modified extensively for general application to gas flow through a porous bed, since the original derivation implied an incompressible fluid. It is, however, quite simple to extend the relation to the special case of isothermal gas flow.

Equation (15) may be rewritten as follows by substituting  $S_{0}$  for  $\frac{\sigma}{m}$  :

$$\frac{Q}{A} = 1033 \text{ g. } \frac{k}{P} \cdot \frac{\varepsilon^3}{(1-\varepsilon)^2} \quad \frac{1}{So^2} \left(-\frac{\delta P}{\delta x}\right)$$

The introduction of the conversion factor 1033 g causes  $\frac{\delta P}{\delta x}$  to represent the macroscopic pressure gradient across the bed in atmospheres rather than in dynes/sq. cm.

Multiplying each side by  $\rho$ , the density of the gas at any point in the bed,

$$\frac{Q\rho}{A} = 1033 \text{ g.} \frac{k}{\mu} \cdot \frac{\epsilon^3}{(1-\epsilon)^2} \frac{\rho}{S_0^2} \left(-\frac{\delta P}{\delta x}\right)$$
 (23)

Let the density of the gas at the given temperature and at a pressure of 1 atmosphere =  $\rho_0$ 

Then, assuming the perfect gas law to be valid,

where P is the pressure of the gas (in atmospheres) at the point under consideration.

Let  $Q \rho = W$ , where W is the mass of gas flowing through the bed per second (constant through the system).

Equation (23) then becomes:

$$\frac{W}{A} = 1033 \text{ g} \quad \frac{k}{\mu} \quad \frac{\epsilon^3}{(1 - \epsilon)^2} \quad \frac{\rho_0 P}{S_0^2} \quad \left(-\frac{\delta P}{\delta \chi}\right)$$

Since  $2P\delta P = \delta P^2$ 

$$\frac{W}{A} = 1033 \text{ g} \quad \frac{k}{\mu} \frac{\epsilon^3}{(1-\epsilon)^2} \frac{\rho_0}{250^2} \left(-\frac{\delta P^2}{\delta \gamma}\right) \tag{24}$$

Let the macroscopic gradient of the square of the pressure across the entire bed =  $\frac{\Delta P^2}{\tau}$  .

Equation (24) then becomes:

$$\frac{W}{A} = 1033 \text{ g.} \quad \frac{k}{\mu} \frac{\epsilon^{3}}{(1 - \epsilon)^{2}} \frac{\rho_{0}}{2S_{0}^{2}} \cdot \frac{\Delta P^{2}}{L}$$
or
$$S_{0} = \sqrt{\frac{1033 \text{ g. k}\rho_{0} \text{ A} \Delta P^{2}}{2\mu \text{ W.L.}}} \cdot \frac{\epsilon^{3}}{(1 - \epsilon)^{2}}$$
(25)

Equation (25) can be simplified to a considerable extent where great accuracy is not required. In the apparatus described in the preceding section, the pressure drop across the bed is normally only a small fraction of the outlet pressure, and the outlet pressure is approximately atmospheric.

Thus 
$$\Delta P^2 = (1 + \Delta P)^2 - 1 \approx 2\Delta P$$
 
$$\frac{\Delta P^2}{2}$$
 may therefore be replaced by  $\Delta P$ , the simple

macroscopic pressure gradient across the bed.

Further, since the rate of gas flow is measured at or near atmospheric pressure,  $\frac{W}{Po} = Q$ .

Equation (25) then becomes:

$$S_0 = \sqrt{\frac{1033 \text{ g k A}\Delta P}{\mu Q L}} \frac{\epsilon^3}{(1-\epsilon)^2}$$
 (26)

By analogy with the liquid permeability coefficient K, a "gas permeability coefficient" G may be defined as follows:

$$G = \frac{QL}{A\Lambda H}$$
 (27)

 $\Delta H$  = pressure drop across bed in centimeters head of gas  $= \frac{1033 \, \Delta P}{P_0} .$ 

Accepting Carman's value of k = 0.20 for the orientation factor, equation (26) becomes:

$$S_0 = 14\sqrt{\frac{\rho_0}{\mu_0}} \frac{\xi^3}{(1-\xi)^2}$$
 (28)

It will immediately be noted that equation (28) is identical in form with equation (18), the Kozeny-Carman relation. This relation may therefore be applied with resonable accuracy to the calculation of gas permeability data, provided that:

- (1) isothermal gas flow is maintained
- (2) the pressure drop across the bed is a small fraction of the outlet pressure

- (3) the outlet pressure is approximately atmospheric
- (4) the flow rate is measured near atmospheric pressure.

Equation (28) is most conveniently expressed by substituting  $G = \frac{QL}{AAH}$   $\frac{QL}{Ah}$   $\frac{P_0}{P_1}$ 

then  $S_0 = 14\sqrt{\frac{A}{\mu L}} \frac{h_1 \rho_1}{Q} \frac{\xi^3}{(1-\xi)^2}$  (29)

Where  $B_0$  = specific surface in sq. cm./cc.

A = cross-sectional area of bed in sq. cm.

 $\mu$  = viscosity of gas in poises

L = depth of bed in cm.

h<sub>1</sub> = pressure drop across the bed in cm. of
liquid (from manometer C, figure 6)

 $\rho_1$  = density of manometer liquid in gm./cc.

Q = gas flow rate in cc./sec., as obtained from manometer D and the flowmeter calibration.

 $\varepsilon$  = porosity of bed.

# (c) Measurements with Corning Fiberglass

Corning fiberglass was chosen for the first comparison of the liquid and gas permeability methods of surface area measurement. Fiberglass strands 1 to 2 meters in length and approximately 0.001 centimeters in diameter were used for both series. of fiberglass 9.9 centimeters in depth was packed into a tube 2.50 centimeters in diameter. Permeability measurements were carried out with air, hydrogen and carbon dioxide. The flowmeter was selected so that the bed and flowmeter manometer readings were of the same order. With each gas, the two manometer readings were recorded for a series of rates of flow, following which the quotients h<sub>1</sub>/Q were calculated from the flowmeter calibration curve. The porosity of the bed was calculated in the usual way from the dimensions of the bed and the weight and density of the fiberglass. The results were as shown in Table VIII.

The values of specific surface obtained with the three gases listed in Table VIII show a maximum deviation of  $\pm 4\%$  from the mean. This deviation is equal to the probable experimental error of the gas permeability measurements.

Liquid permeability measurements were carried out with a bed of similar dimensions to that described above, but using the apparatus and procedure of Part Ia. Entrained air was carefully removed from the bed by repeatedly reducing the pressure above the surface of the liquid. Permeability measurements were carried out with water, benzene and glacial acetic acid, using a fresh bed of fiberglass for each liquid. The results were as shown in Table IX.

TABLE VIII

Gas Permeability Measurements with Corning Fiberglass

Gas	Porosity	Average h <sub>1</sub> /Q	Viscosity (Poises)	Calculated Specific Surface (sq. Cm./cc)
air	0.920	0.837	1.832x10 <sup>-4</sup>	7360
hydrogen	0.920	0.454	0.882xl0-4	7780
carbon dioxide	0.920	0.675	1.51x10-4	7300

True specific surface =  $7000 \pm 400$  sq. cm./cc.

TABLE IX

Liquid Permeability Measurements with Corning Fiberglass

Liquid	Porosity	Average Kv	Calculated Specific Surface (sq. cm./cc.)
water	0.935	5.65x10-4	8200
benzene	0.917	3.55x10-4	7850
acetic acid	0.928	5.73x10-4	7250

True specific surface =  $7000 \pm 400$  sq. cm./cc.

The values of specific surface obtained by the use of liquids (with the exception of acetic acid) are seen to be higher than those calculated from gas permeability data. The differences are, in this case, somewhat greater than the probable error of the measurements.

#### (d) Measurements with Natural Wool

Beds were prepared from woolen yarn to test the correlation between gas and liquid permeability data for a surface quite different to that of glass. The wool fibers were unravelled and cut into lengths of approximately 1 centimeter, and were packed at random into the permeability measuring tubes. The results of measurements with air and benzene on two beds were as shown in Table X. As with glass wool, the specific surface calculated from liquid permeability data was slightly higher than that obtained from gas permeability.

## (e) Measurements with Acetylene Black

The liquid and gas permeability methods were next compared for a material of very large specific surface but of non-fibrous form. Four samples of acetylene black supplied by Shawinigan Chemicals Limited were employed for this purpose.

The beds of acetylene black for the gas permeability measurements were supported on thin pads of fiberglass over the copper gauze in the permeability tube. The resistances

TABLE X

Air and Benzene Permeability Measurements with Wool.

Fluid	Porosity	Average $\frac{h_1\rho_1}{Q\mu}$	Average $K \nu$	Calculated Specific Surface (sq. cm./cc)
air	0.840	1.32x10 <sup>3</sup>		1470
benzene	0.800		9.92x10 <sup>-4</sup>	1590

TABLE XI

Gas permeability Measurements with Acetylene Black

Sample	Gas	Porosity		Calculated Specific Surface (sq. cm./cc)
#1	air	0.984	1.385x104	84,000
#2	oxygen air	0.984 0.946 0.946	1.63x104 4.10x104 6.49x104	133,000 33,000 43,000
#3	oxygen air oxygen	0.895 0.905	1.48x10 <sup>5</sup> 2.43x10 <sup>5</sup>	33,000 54,000
#4	air oxygen	0.850 0.858	2.76x10 <sup>4</sup> 9.11x10 <sup>3</sup>	9,800 5,000

of the pads were first determined by blank runs, and were found in every case to be negligible by comparison with the resistances of the beds. The beds of acetylene black were allowed to settle to constant depths before permeability measurements were commenced, by passing dry gas through the beds at a flow rate higher than the maximum to be used in the measurements. The results of permeability measurements with air and oxygen on the four samples were as shown in Table XI.

The densities of the acetylene black samples were measured by displacement of benzene in a pyknometer flask. The acetylene black was first boiled in the benzene for fifteen minutes to displace air as completely as possible. The mixture was then cooled to room temperature and diluted with benzene to fill the pyknometer bottle. The density values obtained in this way were used in calculating the bed porosities for both gas and liquid permeability runs.

Liquid permeability measurements were carried out with benzene and with water, to which had been added a trace of acetone to facilitate wetting. As before, the beds of acetylene black were supported on thin pads of fiber-glass over the copper gauze. The resistance of each pad was first determined by a blank run, and was subtracted from the resistance (reciprocal of permeability) measured with the actual bed. The beds were prepared by boiling the

TABLE XII

Liquid Permeability Measurements with Acetylene Black

Sample	Liquid	Porosity	Average Kv	Calculated Specific Surface (sq. Cm./cc.)
#1	benzene	0.984	1.43x10 <sup>-5</sup>	225,000
	water	0.984	5.47x10 <sup>-5</sup>	116,000
#2	benzene	0.960	7.42x10-6	120,000
	water	0.964	1.44x10-5	97,000
#3	benzene	0.931	2.83xl0 <sup>-5</sup>	34,000
	water	0.936	3.68xl0 <sup>-5</sup>	33,000
<b>#</b> <sup>1</sup> 4	benzene	0.913	1.96x10 <sup>-5</sup>	32,000
	water	0.890	1.29x10 <sup>-4</sup>	9,100

TABLE XIII

Calculated Specific Surfaces of Acetylene Black Samples

Specific Surface (sq.cm./cc.)

Fluid	Sample #1	#2	#3	#4
Air	84,000	33,000	33,000	9,800
0 <b>xy</b> gen	133,000	43,000	54,000	5,000
Benzene	225,000	120,000	34,000	32,000
Water	116,000	97,000	33,000	9,100

acetylene black in the liquid concerned, reducing the pressure above the liquid repeatedly to remove entrained air, and then decanting the mixture into the permeability tube. The beds were allowed to settle to constant depth before use by running liquid through the bed under the maximum possible head. The results of the liquid permeability measurements were as shown in Table XII.

The specific surfaces calculated from the gas and from the liquid permeability data are summarized in Table XIII for comparison of the two methods. The results are seen to vary in erratic fashion, and indicate only that the specific surfaces decrease from Sample #1 to Sample #4. The values obtained with different fluids for any one sample bear no apparent relation to each other.

## (f) Measurements with Respirator Filter Pads

As mentioned in the introduction, it was originally intended that the establishment of the limits of usefulness of the liquid and gas permeability methods would form the principal subject matter of the investigation.

However, the promising results obtained with fibrous materials of moderate specific surface made it desirable to apply these methods without a rigorous study of their range of validity. It was felt that the liquid and gas permeability methods would provide a valuable tool for examination of materials where efficiency depended in any way on the surface area.

The first materials investigated were a series of seven wool-asbestos respirator filter pads supplied by the National Research Council. No information was made available as to the composition or method of manufacture of these pads. However, the percentage penetration as measured on a smoke penetrometer was indicated on each pad.

Beds were prepared by removing the filter pads from their timplate containers and packing them into permeability tubes with as little disturbance of the original fiber structure as possible. Permeability measurements were carried out with dry air and with benzene in the usual manner. The average densities of the materials of the seven pads were determined by displacement of benzene in the pyknometer flask.

The results of the permeability measurements with air and with benzene were as shown in Tables XIV and XV respectively.

The values of specific surface listed in Table

XV (with the exception of Sample 5) show a steady decrease

with increasing smoke penetration. A similar but less per
fect trend is shown in Table XIV. In both cases the ex
ceptionally high values of specific surface coincide with

high densities of the samples. These high densities pre
sumably indicate high asbestos contents in the filter pads.

Since no details are available as to the percentage composition

Q OS

TABLE XIV

Air Permeability Measurements with Filter Pads

Sample	Penetration (per cent)	Density (gm./cc.)	Porosity	Average hipi	Calculated Specific Surface (sq. cm./cc.)
1234567	.08 .10 .15 .20 .30 .55	1.44 1.42 1.45 1.39 1.51 1.40	0.587 0.581 0.593 0.555 0.595 0.581 0.551	1.825x10 <sup>4</sup> 1.230x10 <sup>4</sup> 1.040x10 <sup>4</sup> 0.924x10 <sup>4</sup> 0.989x10 <sup>4</sup> 1.020x10 <sup>4</sup> 0.564x10 <sup>4</sup>	8900 6800 7900 6600 8300 6800 4500

TABLE XV

Benzene Permeability Measurements with Filter Pads

Sample	Penetration (per cent)	Density (gm./cc.)	Porosity	Average K $ u$	Calculated Specific Surface (sq. cm./cc)
1 2 3 4 5 6 7	.08 .10 .15 .20 .30 .55	1.44 1.42 1.45 1.39 1.51 1.40	0.895 0.905 0.895 0.896 0.888 0.900	1.180x10 <sup>-4</sup> 1.615x10 <sup>-4</sup> 1.360x10 <sup>-4</sup> 1.410x10 <sup>-4</sup> 0.737x10 <sup>-4</sup> 2.60x10 <sup>-4</sup> 3.28x10 <sup>-4</sup>	10,400 10,000 9,700 9,600 12,200 7,900 5,400

of the filters, the problem cannot be analyzed further. However, it seems probable that the specific surface divided by the percentage of asbestos (or some simple function of this quantity) would be found to decrease with increasing smoke penetration.

The values of specific surface calculated from air permeability measurements are in all cases lower than those obtained from liquid permeability data. The differences between corresponding values are in several cases greater than the probable error of the measurements.

#### (g) Measurements with Respirator Charcoal

The gas permeability method of surface area measurement was next investigated as a possible means of grading respirator charcoal. Four charcoal samples were obtained from the National Research Council for this purpose. The samples were identified as follows:

- Sample #1 English coconut charcoal, 2/3 saturated, suitable for military use
- Sample #2 Canadian coconut charcoal, "poor", volume activity approximately 8.
- Sample #3 American coconut charcoal, suitable for military use.
- Sample #4 English briquetted coal charcoal, suitable for civilian use only.

Each sample was partially crushed with a steel roller, after which the broken material was screen-classified. Air permeability measurements were carried out with beds of the original material and of the various

size fractions for each sample. The superficial densities of the original samples were determined by displacement of benzene; the values so obtained were used for all size fractions.

The results of the air permeability measurements with the four samples were as shown in Table XVI.

Two representative size fractions, 28 to 35 mesh and 65 to 150 mesh, were chosen for further investigation. The permeabilities of these fractions to hydrogen and to carbon dioxide were measured for each of the four charcoal samples. The results were as shown in Table XVII.

The specific surface data of Tables XVI and XVII are summarized in Table XVIII to facilitate comparisons of results.

Excluding the original granules and the fractions below 150 mesh, none of which have definite size limits, the specific surfaces are seen to decrease in the order #3, #1, #4 and #2. The only exception occurs with the 28 to 35 mesh fractions and carbon dioxide, where samples #1 and #4 are in reverse order. The differences between the specific surfaces of the various samples are in most cases well beyond the probable error of the measurements. Further, the specific surfaces are found to be in a sequence which is consistent with the information supplied with the charcoal samples.

TABLE XVI

Air Permeability Measurements with Respirator Charcoal

Sample #1 Su	perficial	density = 1.66	gm./cc.
Size Fraction	Porosity	Average $\frac{h_1 \rho_1}{Q_{/}^{\mu}}$	Calculated Specific Surface (sq.cm./cc.)
Original	0.638	1.94x102	150
20 to 28 mesh	0.640	2.72x103	340
28 to 35 "	0.657	4.29x103	480
35 to 65 "	0.658	1.04x104	750
65 to 150 "	0.692	3.56x104	1610
below 150 "	0.675	5.56x105	9600
Sample #2 St	perficial	density = 1.70	gm./cc.
Sample #2 State Size Fraction	perficial Porosity		gm./cc.  Calculated Specific Surface (sq.cm./cc.)
	-		-
Size Fraction	Porosity	Average hip	Calculated Specific Surface (sq.cm./cc.)
Size Fraction Original	Porosity 0.688	Average h202	Calculated Specific Surface (sq.cm./cc.)
Size Fraction Original 20 to 28 mesh	Porosity  0.688  0.632	1.45x10 <sup>2</sup> 2.59x10 <sup>3</sup>	Calculated Specific Surface (sq.cm./cc.)  175 310
Size Fraction Original 20 to 28 mesh 28 to 35 "	0.688 0.632 0.635	Average hapa Qpa 1.45x10 <sup>2</sup> 2.59x10 <sup>3</sup> 2.40x10 <sup>3</sup>	Calculated Specific Surface (sq.cm./cc.)  175 310 430

# TABLE XVI (continued)

Sample #3	Superficial	l density = 1.76	gm./cc.
Size Fraction	Porosity	Average hipi	Calculated Specific Surface (sq.cm./cc.)
Original	0.653	1.73x10 <sup>2</sup>	164
20 to 28 mesh	0.680	2.27x10 <sup>3</sup>	400
28 to 35 "	0.692	3.97x10 <sup>3</sup>	570
35 to 65 "	0.698	8.84x103	870
65 to 150 "	0.705	2.80x104	1870
b <b>elow 150 "</b>	0.725	3.75x105	11,300
Sample #4 Size Fraction	Superficial Porosity	density = 1.70  Average $\frac{h_1\rho_1}{Q_{\rho_1}}$	gm./cc.  Calculated Specific Surface (sq.cm./cc.)
	-		Calculated Specific
Size Fraction	Porosity	Average hipi	Calculated Specific Surface (sq.cm./cc.)
Size Fraction Original	Porosity 0.621	Average h1/01 Q/4	Calculated Specific Surface (sq.cm./cc.)
Size Fraction Original 20 to 28 mesh	0.621 0.635	Average h1/01 Q/4  1.95x10 <sup>2</sup> 2.38x10 <sup>3</sup>	Calculated Specific Surface (sq.cm./cc.) 144 320
Original 20 to 28 mesh 28 to 35 "	0.621 0.635 0.652	Average hapa Qpa 1.95x10 <sup>2</sup> 2.38x10 <sup>3</sup> 4.23x10 <sup>3</sup>	Calculated Specific Surface (sq.cm./cc.)  144  320  470

TABLE XVII

Gas Permeability Measurements with Respirator Charcoal

Sample	Size Fraction	Gas	Porosity	Average $\frac{h_1\rho_1}{Q\mu}$	Calculated Specific Surface (sq.cm./cc.)	
1 2 3 4	28 to 35 " " " " " "	H2 H2 H2 H2	0.679 0.636 0.691 0.651	4.06x103 4.86x103 4.89x103 5.56x103	510 420 580 500	
1 2 3 4	28 to 35 " " " " " "	CO 2 CO 2 CO 2	0.641 0.628 0.682 0.650	4.18x10 <sup>3</sup> 4.99x10 <sup>3</sup> 4.40x10 <sup>3</sup> 5.00x10 <sup>3</sup>	440 420 550 480	-91-
1 2 3 4	65 to 150 " " " " " "	H2 H2 H2	0.685 0.680 0.707 0.693	2.25xl04 2.68xl04 3.53xl04 2.60xl04	1610 1460 1890 1560	
1 2 3 4	65 to 150 11 11 11 11 11 11 11 11	CO 2 CO 2 CO 2	0.692 0.675 0.705 0.675	3.46x104 2.58x104 2.73x104 2.45x104	1590 1350 1850 1410	

TABLE XVIII

Specific Surfaces of Respirator Charcoal Samples (sq.cm./cc.)

Size Fraction	Gas	Sample #3	Sample #1	Sample #4	Sample #2
Original	air	164	150	144	175
20 to 28	air	400	340	320	310
28 to 35	air	570	480	470	430
28 to 35	Нz	580	510	500	420
<b>2</b> 8 to 35	COs	550	440	480	420
35 to 65	air	870	750	710	630
65 to 150	air	1870	1610	1410	1400
65 to 150	Нz	1890	1610	1560	1460
65 to 150	COs	1850	1590	1410	1350
below 150	air	11300	9600	10300	10600

The highest values of calculated specific surface are obtained with the charcoals stated to be suitable for military use, while the lowest specific surface corresponds to the charcoal classified as "poor".

Satisfactory agreement is shown between the values of specific surface obtained by the use of the three different gases with any one fraction. The differences are only of the order of the experimental error, although the specific surfaces may be seen to decrease in the sequence hydrogen, air, carbon dioxide, in the majority of cases.

#### 3. DISCUSSION OF RESULTS

The specific surfaces calculated from liquid and from gas permeability data are in fair agreement for fiberglass, natural wool, and wool-asbestos filter pads. Serious discrepancies, however, are encountered with acetylene black. One or both of the following may be responsible for the lack of agreement: first, the experimental errors involved in dealing with a material possessing the physical characteristics of acetylene black, and second, the limitations of the liquid and gas permeability methods.

Serious errors may be introduced into all of the specific surface calculations as a result of the difficulty of determining the true densities of the acetylene black samples. Since the porosities vary considerably with dif-

ferent beds, the error introduced by the use of an incorrect density value will also vary from run to run. A second source of error, in the liquid permeability determinations, is the incomplete removal of occluded air from the beds of acetylene black. No assurance can be given that the quantity of residual air is reasonably constant with different beds. The most divergent value found in Table XIII, the specific surface of sample #4 measured by the benzene permeability method, may well be attributed to this cause. Table XII shows that the porosities of beds formed in benzene are equal to or less than the porosities of beds formed in water for samples #1, #2 and #3. For sample #4, however, the porosity in benzene is greater than in water, indicating possible voids. A lower porosity for sample #4 would bring the calculated specific surface for benzene into line with those calculated for water and for gases.

The limits of applicability of the permeabilityspecific surface relationship may well be exceeded by acetylene black, since the beds possess specific surfaces and
porosities considerably greater than any investigated hitherto. The present investigations do not give any direct indication of the particle sizes at which these limits are
reached for liquid or for gas permeabilities. However,
some indication of the order of magnitude may be obtained

by consideration of the gas and liquid permeability results for materials of known specific surface.

Stagnant layers of fluid which envelop all solid surfaces in the bed have been considered responsible for the frequently observed fact that calculated specific surfaces are greater than the true specific surfaces. Such layers of stagnant fluid obviously have two effects; first, to decrease the effective porosity of the bed, and second, to decrease the effective specific surface by increasing the average particle size. An approximate analysis of these effects, for a material of simple physical form such as fiberglass, can be made as follows:

Consider the bed of fiberglass to be composed of n cylinders of length 1 and radius r, where r is very small by comparison with 1. Then the true specific surface of the material

$$S_0 = \frac{2\pi r!}{\pi r^2!} = \frac{2}{r} \tag{30}$$

and the volume of material in the bed =  $\pi r^2 \ln$ 

If the total volume of the bed = V, the true porosity of the bed  $\epsilon = \frac{V - \pi r^2 \ln}{V} = 1 - \frac{\pi r^2 \ln}{V}$ 

Assume now that all surfaces are covered by a stationary layer of fluid of effective thickness  $\Delta r$ . Then the effective specific surface  $S_e = \frac{2}{r+\Delta r}$ , and the effective porosity  $\epsilon_e = 1 - \frac{\pi(r+\Delta r)^2 \ln}{V} = 1 - \frac{(r+\Delta r)^2}{r^2} (1-\epsilon)$ .

The effective permeability  $K_e$  measured for this bed must satisfy the equation  $S_e = 14 \sqrt{\frac{1}{K_e \nu}} \frac{\mathcal{E}_e^3}{(1 - \mathcal{E}_e)^2}$ 

Therefore 
$$\frac{2}{\mathbf{r}+\Delta \mathbf{r}} = 14 \sqrt{\frac{1}{\mathbf{K}e^{\nu}}} \left[ \frac{1-\frac{(\mathbf{r}+\Delta\mathbf{r})^2}{\mathbf{r}^2} (1-\epsilon)}{\left[\frac{(\mathbf{r}+\Delta\mathbf{r})^2}{\mathbf{r}^2} (1-\epsilon)\right]^2} \right]$$

Solving for  $K_e \nu$ 

$$K_{\theta} \nu = \frac{49(r+\Delta r)^2 \left[1 - \frac{(r+\Delta r)^2}{r^2} (1-\epsilon)\right]^3}{\left[\frac{(r+\Delta r)^2}{r^2} (1-\epsilon)\right]^2}$$
(31)

Let  $S_{\rm C}$  represent the specific surface which would be calculated from this effective permeability, without prior knowledge of the stationary layer.

Then 
$$S_e = 14 \sqrt{\frac{1}{K_e \nu} \frac{\epsilon^3}{(1-\epsilon)^2}}$$

Substituting the value of  $K_{e}\nu$  from equation (31)

$$S_{e} = \frac{2(r+\Delta r)}{r^{2}} \sqrt{\frac{\varepsilon^{3}}{\left[1 - \frac{(r+\Delta r)^{2}}{r^{2}} (1 - \varepsilon)\right]^{3}}}$$
(32)

From equations (30) and (32), the ratio of the calculated specific surface  $S_{\mathbf{c}}$  to the true specific surface  $S_{\mathbf{0}}$  is as follows:

$$\frac{S_{c}}{S_{0}} = \frac{r+\Delta r}{r} \sqrt{\left[1 - \frac{(r+\Delta r)^{2}}{r^{2}} (1-\epsilon)\right]^{3}}$$

Therefore 
$$\left[1 - \frac{(r + \Delta r)^2}{r^2} (1 - \epsilon)\right]^3 \frac{r^2}{\epsilon^3 (r + \Delta r)^2} = \left(\frac{S_0}{S_c}\right)^2$$

For a first approximation, where  $\varepsilon > 0.9$ ,

$$\left[1 - \frac{3(r+\Delta r)^2}{r^2}(1 - \varepsilon)\right] \frac{r^2}{\varepsilon^3(r+\Delta r)^2} = \left(\frac{S_0}{S_0}\right)^2$$

Solving for  $\frac{r+\Delta r}{r}$ 

$$\frac{\mathbf{r} + \Delta \mathbf{r}}{\mathbf{r}} = \frac{1}{\sqrt{\varepsilon^3 \left(\frac{S_0}{S_c}\right)^2 - 3\varepsilon + 3}}$$
 (33)

Equation (33) enables an estimate to be made of the effective thickness of the stationary fluid layer, knowing the true radius or specific surface of the cylindrical particles, the true porosity of the bed, and the specific surface calculated from a permeability determination with the fluid in question.

A calculation of the thickness of the stationary layer for each of the fluids in Tables VIII and IX is not justifiable, since the true specific surface of the fiber-glass is not known with sufficient accuracy. However, taking the most extreme case, the specific surface calculated from water permeability data is \$200 sq. cm./cc., while the mean value of the true specific surface is 7000 sq. cm./cc. The radius of the equivalent cylindrical particle is 2.9 x 10<sup>-4</sup> centimeters, the true porosity of the bed 0.935. Equation (33) then indicates that a stationary layer of water 4 x 10<sup>-5</sup> centimeters in thickness is present.

This result supports the view taken by Lea and Nurse (37) that the stagnant layers are of much greater than

molecular thickness. It further indicates that the limit of applicability of the water permeability method of surface area measurement has been reached. The following errors are introduced into measurements with beds of long cylindrical particles of the above porosity (0.935) by a stationary layer  $4 \times 10^{-5}$  centimeters in thickness:

Radius of Cylinders (cm.)	True Speci Surface (sq.	fic Error i cm./cc.) Specif	n Calculated ic Surface
2 x 10 <sup>-3</sup>	1000	3%	
4 x 10-4	5000	14%	
2 x 10 <sup>-4</sup>	10,000	28%	
4 x 10-5	50,000	120%	

Errors of the same order as those listed above are also introduced into specific surface calculations with spherical particles. Consequently, water permeability measurements with a material such as acetylene black are virtually meaningless. It may be noted that a similar situation was found by Lea and Nurse, who concluded that liquid permeability measurements were suitable only for powders of specific surface less than 1000 sq. cm./cc.

No attempt was made in the preceding analysis to estimate the thicknesses of the stagnant layers for other liquids or gases, since the accuracy of the measurements did not justify such calculations. However, certain qualitative observations can be made for these fluids. The values of calculated specific surface for the material with the simplest

physical form, Corning fiberglass, decrease successively with the following fluids: water, benzene, hydrogen, air, carbon dioxide, acetic acid. The true specific surface, as estimated from microscopic examination, is equal to or slightly less than that calculated from acetic acid permeability.

Various portions of this sequence are reproduced in measurements with other solids. The series hydrogen, air, carbon dioxide is found with six out of eight samples of respirator charcoal. The specific surfaces calculated from benzene permeability measurements with natural wool and with wool-asbestos filter pads are in all cases greater than those calculated from air permeability measurements. The specific surfaces calculated from water permeability measurements with sand beds are, in turn, greater than those calculated from benzene permeability measurements. The only portion of the sequence without independent confirmation is the position of the lowest member, acetic acid.

The above sequence provides experimental evidence for the postulate that stagnant gas films are thinner than the corresponding liquid films. Acetic acid may be a true exception; however, in view of the limited data, this anomaly is more probably the result of experimental error. The relative thinness of the gas films signifies that gas permeability methods may be used for higher specific surface ranges than liquid permeability methods. While the present

investigations do not aid in locating the upper limit for the gas permeability method, it is apparent from the measurements with fiberglass that this limit is well in excess of 7000 sq. cm./cc.

The results obtained with respirator filter pads and charcoal indicate that permeability methods may be useful for purposes other than actual measurement of specific The calculated specific surfaces of the respirator filter pads may be correlated with the smoke penetration values, as mentioned under section 2 (f). calculated specific surfaces for the respirator charcoal samples fall into a sequence which corresponds with the descriptions of the samples given under section 2 (g). latter correlation is particularly striking when it is considered that the permeability method can measure only the "friction surface" of the constituent particles. The only portion of the surface which can affect the measured permeability is that which can be traversed by the streamlines of the fluid; deep pockets and marrow cracks can have little or no effect. Thus, the differences in total specific surface of the four samples are undoubtedly far larger than those indicated by the calculated values. This factor limits the usefulness of the gas permeability method for grading respirator charcoal, since the sensitivity of the measurements cannot be great. However, its ease of application may recommend it for certain purposes.

#### BIBLIOGRAPHY

- 1. J. Kozeny 1927 Sitzber. Akad. Wiss Wien. Math Naturw. Klasse, Abt. IIa, 136 271-306
- 2. J. Kozeny 1927 Wasserkraft und Wasserwirtschaft, 22, 67
- 3. P.C. Carman 1937 Trans. Inst. Chem. Engrs. 15, 150-166
- 4. P.C. Carman 1938 J. Soc. Chem. Ind., 57, 225-234
- 5. H. Heywood 1938 Proc. Inst. Mech. Engrs. 140, 257
- 6. L.A. Wagner 1933 Proc. Am. Soc. Testing Materials 33 (II), 553
- 7. A.H.M. Andreasen 1929 Kolloid-Z., 49, 48, 252 1930 Zement, 19, 698
- 8. W.F.Carey and C.J. Stairmand 1938 Trans. Inst. Chem. Engrs., 16, 57
- 9. P.S. Roller 1932 Proc. Am. Soc. Testing Materials, 32 (II) 607
- 10. G. Marten, C.E. Blyth and H. Tongue 1923-24 Tran. Ceram. Soc., 23, 61
- 11. Munroe, 1931 Ph.D Thesis
- 12. Tunstall 1933 Proc. Inst. Mech. Engrs., 125, 455
- 13. P.J. Askey and C.G.P. Feachem
  1938 J. Soc. Chem. Ind., 57, 272-276
- 14. H.P.G. Darcy 1856 "Les Fontaines Publiques de la Ville de Dijon", Victor Dalmont, Paris
- 15. S.L. Bigelow 1907 J. Amer. Chem. Soc., 29, 1675-1693
- 16. P.C. Carman 1934 J. Soc. Chem. Ind., <u>53</u>, 159-166T, 301-309T
- 17. Brunhes 1897 "Recherches Experimentales sur la Filtration"

- Karl Schaum 1924 Kolloid-Z., 34, 1
- 18. G.H. Fancher and J.A. Lewis
  1933 Ind. Eng. Chem, 25, 1139-1147
- 19. R.N. Traxler and L.A.H. Baum 1936 Physics, 7, 9-14
- 20. M. Muskat 1937 "The Flow of Homogeneous Fluids
  Through Porous Media" McGraw-Hill
  Book Co., 56, 130
- 21. M. Muskat Ibid., 69
- 22. O. Emersleben 1925 Physik. Z., 26, 601-610
- 23. Darapsky 1912 Z. Math. Physik., 60, 170
- 24. A.J.E.J. Dupuit

  1863 "Études Théoretiques et Pratiques sur le Mouvement des Eaux", Paris
- 25. A.G. Greenhill 1881 Proc. London Math. Soc., 13, 43
- 26. F.E.Bartell and H.J. Osterhof 1928 J. Phys. Chem., 32, 1553-1571
- 27. D.I. Hitchcock 1926 J. Gen. Physiol., 2, 755-762
- 28. J.L. Fowler and K.L. Hertel
  1940 J. Applied Phys., II, 496-502
- 29. R.R. Sullivan and K.L. Hertel
  1940 J. Applied Phys., 11, 761-765
- 30. W. Schriever 1930 Trans. Am. Inst. Mining Met. Engrs., (Petroleum Div.) 86, 329-336
- 31. M. Muskat 1937 "The Flow of Homogeneous Fluids Through Porous Media" McGraw-Hill Book Co., 79-80
- 32. J. Donat 1929 Wasserkraft und Wasserwirtschaft, 24, 225-229
- 33. C.A. Coulson 1935 Univ. of London, Ph.D. Thesis
- 34. S.P. Burke and W.B. Plummer 1928 Ind. Eng. Chem., 20, 1196-1200

- 35. T.H. Chilton and A.P. Colburn
  1931 Ind. Eng. Chem. 23, 913-919
- 36. P.C.Carman 1939 J. Soc. Chem. Ind., 58, 1-7
- 37. F.M. Lea and R.W. Nurse
  1939 J. Soc. Chem. Ind., <u>58</u>, 277
- 38. G. Bozza and I. Secchi 1929 Giorn. Chem. Ind. Applicata, 11, 443, 487
- 39. H.Green and G.A. Ampt.
  1912-13 J. Agr. Sci., 5, (Part 1) 1-26

## PART II

Problems of Explosives Production

Preparation of Carbamite from Crude Ethylaniline

#### 1. INTRODUCTION

Carbamite (sym.-diethyl carbanilide) is widely used as a moderant for coating progressive-burning propellants. The method of preparation normally employed involves the reaction of ethylaniline with phosene according to the equation:

2 
$$\bigcirc$$
 NHC<sub>2</sub>H<sub>5</sub> + COCl<sub>2</sub>  $\longrightarrow$   $\bigcirc$  NC<sub>2</sub>H<sub>5</sub>COC<sub>2</sub>H<sub>5</sub>N $\bigcirc$  + 2 HCl

Shortages of pure ethylaniline developed in Canada during the year 1940 as a result of the rapidly expanding production of propellants for military use. The manufacture of ethylaniline was undertaken by the Dye and Chemical Co., of Canada, and efforts were initiated to use this material for the production of carbamite.

The raw material supplied by the manufacturer contained approximately 7% of aniline, 85% of monoethylaniline, and 8% of diethylaniline. The following reactions were expected to occur on treatment of this material with phospene:

(a) The aniline would react with phosgene to form carbanilide according to the equation:

(b) The monoethylaniline would react with phosgene to form sym.-diethyl carbanilide:

2 
$$\bigcirc$$
 NHC<sub>2</sub>H<sub>5</sub> + COCl<sub>2</sub>  $\longrightarrow$   $\bigcirc$  NC<sub>2</sub>H<sub>5</sub>COC<sub>2</sub>H<sub>5</sub>N  $\bigcirc$  + 2 HCl

In addition, a number of side reactions would occur at elevated temperatures and in the presence of an excess of phosgene. One of these would result in the formation of phenyl isocyanate:

The characteristic odor of this compound would therefore be a useful indication of local overheating or excess of phosgene.

(c) The diethylaniline would undergo no reaction with the phosgene but would absorb a part of the hydrogen chloride evolved by reactions (a) and (b)

The investigations to be described in the succeeding paragraphs are primarily applications of established industrial procedures for the manufacture of carbamite.

Both the du Pont and Imperial Chemical Industries processes are applied to the crude ethylaniline supplied by the Canadian Dye and Chemical Co. An important phase of the investigation is the separation of the desired carbamite from the carbanilide and other by-products of the reaction.

#### 2. EXPERIMENTAL PROCEDURE AND RESULTS

### (a) Du Pont Process

Details of the manufacturing process for carbamite used by E. I. du Pont de Nemours and Co. were obtained through the courtesy of Canadian Industries Limited. In this process, a mixture of 550 pounds of pure monoethylaniline and 850 pounds of diethylaniline, cooled to 15°-17°C., is treated with 228 pounds of phosgene. The phosgene is blown over the surface of the mixture in an enamelled kettle. The temperature is allowed to rise to 35°-40°C. during the The reaction mixture is held at this temabsorption. perature for 1 hour after the addition of the phosgene, then is heated to 100°C. and held at the higher temper-The contents of the kettle are next ature for 1 hour. blown into a tank containing 10,000 pounds of cold water; 127 pounds of 93% sulphuric acid are added with thorough agitation, and the mixture is allowed to cool to 35°C. The product, which should solidify at this point, is filtered off and washed free from acid. The acid solution contains the diethylaniline, which is recovered by neutralization with sodium carbonate.

A preliminary trial of the above procedure was carried out with a mixture of 10 grams of pure monoethylaniline and 15.5 grams of diethylaniline. Phosgene was condensed in a calibrated receiver cooled by dry ice and

acetone; 4.2 grams of gas were distilled into the mixture of bases, contained in a large test tube cooled to 15°C. After heating by the prescribed schedule, a product was obtained which consisted of a brown oil together with crystals of diethylaniline hydrochloride. The crystals were dissolved when the mixture was poured into water and acidified, leaving a light colored oil which gradually solidified on stirring. The solid product was recrystallized from alcohol, yielding nearly white crystals of melting point 70° to 71°C.

The du Pont method was next applied to the crude ethylaniline supplied by the Dye and Chemical Co. of Canada. The procedure described in the preceding paragraph was carried out with a mixture of 11.7 grams of crude ethylaniline (containing 10 grams of pure monoethylaniline) and 14.6 grams of diethylaniline. The reaction mixture was poured into water and acidified, yielding a dark brown oil which solidified to a pasty mass of crystals after prolonged The crystals were freed from oil by pressing on stirring. a suction filter and washing repeatedly with small quantities of alcohol. The solid residue was recrystallized from hot alcohol, yielding a product melting at 236°C. This material evidently consisted of carbanilide produced from the aniline in the raw material. The expressed oil and alcohol washings from the carbanilide were united and brought to a

clear solution by the addition of further alcohol. Slow removal of alcohol on a steam bath yielded a crystalline product of melting point 71°C., identified as carbamite.

The third test was carried out to determine the yield of purified carbamite from crude ethylaniline. this purpose, a mixture of 31 grams of crude ethylaniline and 40 grams of diethylaniline was treated with the theoretical quantity (11.9 grams) of phosgene. As before. a pasty mass of crystals was obtained by pouring the reaction mixture into water and acidifying. This mass was washed with water, pressed dry on a suction filter, and The dry product was then dissolved in alcohol. weighed. The carbanilide was precipitated by careful evaporation and cooling and was separated by filtration. The clear alcoholic solution was allowed to crystallize, following which the crystals of carbamite were separated, dried and weighed.

The aqueous solution containing diethylaniline and unreacted ethylaniline in the form of sulphates and hydrochlorides was made alkaline with sodium carbonate. The layer of free bases was separated, and the remaining solution was extracted with ether. The bases were recovered from the ether extract by evaporation and were united with the separated layer.

The yields obtained were as follows:
Weight of crude carbamite = 9.8 grams
Weight of purified carbamite = 8.9 grams

Weight of recovered bases = 50.2 grams

Weight of unreacted ethylaniline (assuming 100% recovery of diethylaniline) = 7.7 grams

Theoretical yield of carbamite = 20.2 grams

Actual yield = 44% of theoretical.

A larger scale test was made with 54.5 grams of crude ethylaniline, 68 grams of diethylaniline, and 19.5 grams of phosgene. Attempts were made in this test to separate the final product of oil and crystals by selective Both oil and crystals appeared to be solvent action. equally soluble in benzene, carbon tetrachloride, chloroform, alcohol, alcohol-water mixtures, and glacial acetic acid. Some degree of separation was obtained with acetone and with Skelly Solve A, the oil being slightly more soluble than the crystals in both solvents. In addition, the rate of solution of the oil was appreciably greater than that of the Repeated washings of the mixture of oil and crycrystals. stals with small quantities of Skelly Solve A on a suction filter yielded clean crystals of carbamite and carbanilide. However, evaporation of the washings revealed that a considerable quantity of carbamite had been lost with the oil.

A still larger scale trial was made with 227 grams of crude ethylaniline, 280 grams of diethylaniline, and 80 grams of phosgene. The reaction was carried out in a one-liter round bottomed flask fitted with a small motor driven stirrer. Great difficulty was experienced in prevented local

overheating of the reaction mixture. Before the addition of phosgene was complete, the mass had become too stiff for effective agitation with the small stirrer.

A strong odor of phenyl isocyanate was observed during the latter stages of the reaction. The reaction product after acidification contained an unusually high proportion of oil and was colored a deep blue. The separation of the carbamite was consequently laborious, and the yield of purified product was very low.

An attempt was finally made to reduce the proportion of undesirable by-products by purification of the raw material. On subjecting the crude ethylaniline to simple distillation, a first cut comprising water and a deep yellow oil of strong sulphur odor was obtained in the vicinity of 100°C. The main cut was obtained as a pale yellow oil with a boiling range of 196° to 208°C. Finally, small amounts of dark colored material distilled, leaving a tarry residue which could not be vaporized without pyrolysis.

The main cut from the preliminary distillation was then subjected to fractional distillation with a short column. The first fraction, consisting of a pale yellow oil of strong sulphur odor, distilled between 90° and 100°C. The principal fraction was obtained as a colorless oil of boiling range 196° to 206°C., comprising nearly 80% of the

original material. A small quantity of dark oily residue remained in the distillation flask.

A mixture of 26 grams of purified ethylaniline and 40 grams of diethylaniline was treated with phosgene in the usual way. The resulting product after acidification was much lighter in color and separated more readily than that prepared from crude ethylaniline. Appreciable amounts of oil were still present in the separated material, but were completely removed by pressing and subsequent recrystallization from alcohol.

## (b) I. C. I. Method of Preparation

The procedure employed by Imperial Chemical Industries Ltd., avoids the use of diethylaniline. Sodium carbonate solution is added to the ethylaniline in sufficient quantity to convert the HCl evolved by the reaction to NaCl and NaHCOs. A small scale test of this procedure with crude ethylaniline was conducted as follows.

A saturated aqueous solution of 25.5 grams of sodium carbonate was added to 31 grams of crude ethylaniline. The theoretical quantity of phosgene was bubbled into the aqueous layer and allowed to rise through the ethylaniline. Absorption appeared to be rapid and complete. As in the du Pont procedure, the reaction mixture was held at a temperature of 35° to 40°C. for one hour, then heated to 100°C for one hour. The mixture was finally poured into cold water and acidified with sulphuric acid.

A semi-solid product was obtained which was separated and pressed on a suction filter. The dry material was washed with Skelly Solve A, dissolved in alcohol, and recrystallized. Light colored crystals of carbamite of melting point 72°C. were obtained.

Yield of pure carbamite = 14.5 grams

Theoretical yield = 28.5 grams

Actual yield = 50.1% of theoretical

# (c) <u>Purification of Crude Carbamite by Vacuum Distillation</u>

The mixtures of oil and crystals obtained in several of the preceding preparations were united and subjected to vacuum distillation, as a possible means of purification. The resulting distillate was a clear, pale yellow oil which quickly solidified to a crystalline mass. The solid product was dissolved in a little alcohol and allowed to crystallize. White crystals of carbamite of melting point 72.5°C. were obtained.

## (d) Removal of Aniline from Crude Ethylaniline

An attempt was made to remove aniline from the crude ethylaniline by preferential reaction with phosgene. (Complete removal of aniline as carbanilide at this point would avoid the later separation of carbanilide and carbanite.) A quantity of phosgene sufficient to convert

the aniline content to carbanilide was passed into 50 grams of crude ethylaniline at 20°C. A completely liquid reaction product was obtained. Separation of carbanilide could not be achieved by repeated cooling, agitation, or seeding with carbanilide crystals.

## (e) Preparation of Carbamite from Diethylaniline

The following reaction is reported to occur with dimethylaniline at temperatures near its boiling point:

By analogy, it was hoped that the diethylaniline content of crude ethylaniline could be converted to carbamite and ethyl chloride, thus avoiding the problem of disposing of the accumulated diethylaniline.

An excess of phosgene was passed into 30 grams of crude ethylaniline heated to 200°C. When absorption of phosgene had ceased, the product was cooled and poured into water. A dark viscous liquid was obtained which could not be crystallized by repeated cooling, by agitation or by seeding with carbamite crystals. Extraction of the viscous liquid with ether yielded a lighter oil which likewise failed to crystallize. Both lighter and heavier fractions possessed a strong odor of phenyl isocyanate.

#### 3. DISCUSSION OF RESULTS

The du Pont procedure, employing diethylaniline for removal of hydrogen chloride from the reaction, appears to be directly applicable to crude ethylaniline without preliminary treatment. However, a more easily purified product is obtained if the crude ethylaniline is first subjected to a stripping process for removal of sulphur compounds. This preliminary treatment would probably be advantageous on an industrial scale if suitable distillation equipment were available.

bonate solution for diethylaniline, also appears to be applicable to the crude ethylaniline. The product obtained in the present investigation was of equal purity and comparable yield to that obtained by the du Pont method. The I. C. I. method has the advantage of eliminating the use and subsequent recovery of larger quantities of diethylaniline. Further, the presence of the aqueous layer aids in controlling the reaction temperature.

If crude ethylaniline (or ethylaniline stripped free of sulphur compounds) is employed as the starting material, carbanilide and carbamite must be separated in the reaction product. This may be accomplished through the low solubility of carbanilide in cold ethyl alcohol. Alternatively, the separation may be avoided by removing

aniline from the crude ethylaniline before use. The preferential reaction of aniline with phosgene does not appear to be suitable for this purpose. Fractional distillation could probably be employed but would require more elaborate distillation equipment than for removal of sulphur compounds only.

The methods of purifying the crude carbamite require further investigation before use on an industrial scale. Either vacuum distillation of the crude product or pressing on a filter followed by recrystallization from alcohol is reasonable satisfactory on a laboratory scale. However, neither of these procedures are directly applicable to quantity production.

The avoidance of local overheating or excess of phosgene in the reaction mixture by means of adequate stirring appears to be of primary importance. Neglect of these factors results in side reactions which render the purification of the carbamite very difficult. An immediate indication of overheating is given by evolution of the characteristic odor of phenyl isocyanate.

The relatively low yield of carbamite in the present tests may be partially attributed to the small scale of the experiments with the accompanying mechanical losses. The proportion of unreacted ethylaniline is also high, as a result of the inefficient means available for

dispersing phospene through the reaction mixtures.

It is probable that both of these losses could be considerably reduced on an industrial scale.